Journal of Hydrology 611 (2022) 128016

Contents lists available at ScienceDirect

Journal of Hydrology

journal homepage: www.elsevier.com/locate/jhydrol

Research papers

Seasonal fog enhances crop water productivity in a tropical rubber plantation

Palingamoorthy Gnanamoorthy [a], Qinghai Song [a,b,*], Junbin Zhao [c], Yiping Zhang [a,b,*], Jing Zhang [a,d], Youxing Lin [a,b], Liguo Zhou [a,b], Sadia Bibi [a], Chenna Sun [a,d], Hui Yu [a,d], Wenjun Zhou [a,b], Liqing Sha [a,b], Shusen Wang [e], S. Chakraborty [f], Pramit Kumar Deb Burman [f,g]

[a] CAS Key Laboratory of Tropical Forest Ecology, Xishuangbanna Tropical Botanical Garden, Chinese Academy of Sciences, Menglun 666303, China
[b] Center of Plant Ecology, Core Botanical Gardens, Chinese Academy of Sciences, Menglun 666303, China
[c] Department of Biogeochemistry and Soil Quality, Division of Environment and Natural Resources, Norwegian Institute of Bioeconomy Research, 1433 Ås, Norway
[d] University of Chinese Academy of Sciences, Beijing 100049, China
[e] Canada Centre for Remote Sensing, Natural Resources Canada, Ottawa K1A0Y7, Canada
[f] Indian Institute of Tropical Meteorology, Ministry of Earth Sciences, Pune 411008, India
[g] Department of Atmospheric and Space Sciences, Savitribai Phule Pune University, Pune 411007, India

ARTICLE INFO

This manuscript was handled by Marco Borga, Editor-in-Chief, with the assistance of Lixin Wang, Associate Editor

Keywords:
Canopy conductance
Evapotranspiration
Eddy covariance
Net ecosystem CO_2 exchange
Sap flow
Transpiration

ABSTRACT

The rapid conversion of tropical rainforests into monoculture plantations of rubber (*Hevea brasiliensis*) in Southeast Asia (SEA) necessitates understanding of rubber tree physiology under local climatic conditions. Frequent fog immersion in the montane regions of SEA may affect the water and carbon budgets of the rubber trees and the plantation ecosystems. We studied the effect of fog on various plant physiological parameters in a mature rubber plantation in southwest China over 3 years. During the study period, an average of 141 fog events occurred every year, and the majority occurred during the dry season, when the temperature was relatively low. In addition to the low temperature, fog events were also associated with low vapor pressure deficit, atmospheric water potential, relative humidity and frequent wet-canopy conditions. We divided the dry season into cool dry (November-February) and hot dry (March-April) seasons and classified days into foggy (FG) and non-foggy (non-FG) days. During the FG days of the cool dry season, the physiological activities of the rubber trees were suppressed where carbon assimilation and evapotranspiration showed reductions of 4% and 15%, respectively, compared to the cool dry non-FG days. Importantly, the unequal declines in carbon assimilation and evapotranspiration led to enhanced crop water productivity (WP_c) on cool dry FG days but insignificant WP_c values were found between FG and non-FG days of the hot dry season. Our results suggest that, by regulating plant physiology, fog events during the cool dry season significantly reduce water demand and alleviate water stress for the trees through improved WP_c.

1. Introduction

The montane areas (>300 m elevation) of Southeast Asia (SEA) are rich in natural resources and considered to be one of the global biodiversity hotspots and important regions of primary forest carbon stock (Fox et al., 2014; Blagodatsky et al., 2016). However, in recent decades, these areas have been experiencing severe biodiversity loss and environmental risks due to the conversion of natural tropical rainforests into monoculture plantations of rubber (*Hevea brasiliensis*) (Myers et al., 2000; Tan et al., 2011; Zakari et al., 2020). For example, in the southwest edge of China (Xishuangbanna), rubber trees were first introduced in the late 1950s, and its land coverage reached 22% by 2010, forming a new 'non-traditional' environmental area (Zhu et al., 2004; Xu et al., 2014; Giambelluca et al., 2016). Such large-scale changes in land-use patterns in natural forests have led to serious environmental problems that have affected the regional and local forest carbon (Blagodatsky et al., 2016; Warren-Thomas et al., 2018) and water balances (Tan et al., 2011; Pfeifer et al., 2016). Predominantly, the rubber plantations reduce groundwater recharge due to the high rainwater runoff (Ma et al., 2019) and also introduce pollution due to

* Corresponding authors.
E-mail addresses: sqh@xtbg.ac.cn (Q. Song), yipingzh@xtbg.ac.cn (Y. Zhang).

https://doi.org/10.1016/j.jhydrol.2022.128016
Received 8 December 2021; Received in revised form 4 May 2022; Accepted 30 May 2022
Available online 7 June 2022

fertilizer and pesticide applications (Zakari et al., 2020). Further, owing to their larger xylem vessels and comprehensive root system, rubber trees consume more water than rainforest trees (Isarangkool Na Ayutthaya et al., 2011; Tan et al., 2011; Yang et al., 2020), making them more vulnerable to drought. Consequently, a much higher rate of canopy evapotranspiration (ET_c) was found in rubber plantations than in the local natural ecosystems (Guardiola-Claramonte et al., 2010; Tan et al., 2011; Giambelluca et al., 2016). The ET_c was significantly lower during the dry season than in the wet season due to drought and defoliation patterns (Isarangkool Na Ayutthaya et al., 2011; Kobayashi et al., 2014; Niu et al., 2017; Hardanto et al., 2017; Lin et al., 2018a,b; Röll et al., 2019).

During the dry season, fog events occur frequently in Xishuangbanna as in many mountainous ecosystems (Bruijnzeel, 2001). The moisture input from the fog is believed to partially relieve the stresses from lower temperatures and drought of the dry season (Zhang et al., 2014; Fu et al., 2016), thereby allowing high rubber production in this region (Priyadarshan, 2011). These fog events can influence the carbon, water and energy budgets of the ecosystem in various ways. For example, the fog maintains water in plants and soils by reducing transpiration through frequent leaf wetting (Bruijnzeel, 2001; Alvarado-Barrientos et al., 2014; Berry et al., 2014; Gerlein-Safdi et al., 2018a). At the same time, the foliar uptake of fog water can diminish the leaf water deficit and enhance leaf gas-exchange rates (Berry et al., 2014; Baguskas et al., 2017), which in turn lead to ecosystem rehydration in a dry environment (Eller et al., 2013). The foggy (FG) days can enhance the ecosystem productivity because the fog-diffused light can be used by plants for photosynthesis (Mercado et al., 2009; Berry et al., 2014). However, some studies also reported that leaf wetting can weaken photosynthetic carbon assimilation during a dense fog event even under the presence of adequate sunlight (Zhang et al., 2014; Gerlein-Safdi et al., 2018b; Bittencourt et al., 2019). Furthermore, changes in the environmental conditions, such as air temperature (Tair), net radiation (Rn), photosynthetically active radiation (PAR), relative humidity (RH) and vapor pressure deficit (VPD), during fog events can also have a substantial influence on ecosystem water use and productivity (Ritter et al., 2009, 2017; Baguskas et al., 2018). Overall, the responses of both carbon uptake and evapotranspiration to fog can vary among ecosystems with different tree species. For rubber plantations, it is still not clear how changes in productivity and evapotranspiration during fog events affect the ecosystem water-use efficiency, which to a large extent defines their vulnerability to drought stress during the dry season.

The importance of fog in forest ecosystems has been recognized and debated for centuries (Hales, 1757; Stone, 1957), but it is only in recent years that the development of new techniques, such as high-precision gas exchange measurements, xylem sap flow and stable isotopes, has allowed us to investigate the effect of fog on water and carbon processes in different ecosystems (Bruijnzeel et al., 2011; Zhang et al., 2014; Alvarado-Barrientos et al., 2014; Chu et al., 2014; Gotsch et al., 2014; Baguskas et al., 2018; Gerlein-Safdi et al., 2018a,b; Bittencourt et al., 2019). However, the extent to which the leaves of rubber plants can maintain net CO_2 assimilation in the fog season is not known. We need to study the degree of rubber plant physiology responses to different fog and cloud regimes, from FG to cloudy and non-foggy (non-FG) days, in a systematic manner. Therefore, our goal was to understand the effects of fog occurrence on net ecosystem CO_2 exchange (NEE), gross primary production (GPP), ET_c, ecosystem-level crop water productivity (WP_c), canopy conductance (Gs) and stand-level tree transpiration rate (T_c) by analyzing carbon/water flux data during 2014–2016 in a rubber plantation. The specific objectives of the study were to:

- characterize the local fog occurrence in Xishuangbanna rubber plantations;
- reveal changes in environmental conditions as the fog occurs; and
- compare NEE, GPP, ET_c, WP_c, Gs and T_c under FG and non-FG days of cool and hot dry seasons to reveal the impact of fog on these carbon and water processes.

The present study has great implications for the study of the effect of fog on water and carbon cycle in rubber plantations in wide areas of SEA.

2. Materials and methods

2.1. Site description

The study site was located in the experimental area of the Xishuangbanna Tropical Botanical Garden (21°55′30″N, 101°15′59″E; size: ~20 ha; elevation: 570 m a.s.L.), Xishuangbanna, Yunnan Province, southwest China (Fig. S1). It has a hilly terrain. This experimental rubber plantation site was established in 1982 by the Chinese Academy of Sciences (CAS) to study the impact of commercial expansion of rubber plantations on the local area. The tree density of the site was 346 trees/ha with a mean canopy height of ~ 22 m and a mean diameter at breast height (DBH) of 31 cm (Zhao et al., 2014; Lin et al., 2016, 2018a, 2018b). The main rubber-tapping period is May–November (Song et al., 2014). Mineral fertilizer was applied twice in a year (April and July) with an application rate of 75 kg N ha^{-1} yr^{-1} (containing 15% N as $(NH_2)_2CO$, 15% P as $NH_4H_2PO_4$ and 15% K as KCl) (Zhou et al., 2016). The climatic conditions of the study region are controlled by the monsoon regime, with tropical southern monsoon from the equatorial Indian Ocean during May–October forming the humid and hot-wet season. The dry season lasts from November to April of the following year, and it is divided into cool dry season (November–February) and hot dry season (March–April), with winds from the southeastern direction (Tan et al., 2010). The cold air from the southern edges of the subtropical jet streams dominates the dry season (Cao et al., 1996; Tan et al., 2010), causing frequent fog events particularly at night and in the early morning (Liu et al., 2004). Fog events are less frequent in the wet season due to deep orographic convection, which has been seen in several mountain ecosystems around the world (Eugster et al., 2006; García-Santos and Bruijnzeel, 2011; Alvarado-Barrientos et al., 2014). The mean annual rainfall was 1,492 mm over the past 50 years, and ~ 87% of the rainfall occurred during the wet season (Tan et al., 2010). The soil texture is clay-loamy and belongs to the taxonomy group of latosol. The quantity of sand, silt and clay in the top 10 cm soil layer was 40%, 31% and 28%, respectively. The top 10 cm of soil had a pH of 5.11 and a bulk density of 1.42 g cm^{-3} (Balasubramanian et al., 2020). At depths of 0–20, 20–60 and 60–120 cm, the soil moisture (SM, volumetric) at field capacity was 33%, 30% and 27%, respectively (Jiang et al., 2019). In the rubber plantations of this region, the SM during the dry season reaches close to permanent wilting point, and they face severe soil drought in the subsoil layer, particularly during the late dry season (Vogel et al., 1995; Chen and Cao, 2008; Liu et al., 2014a).

2.2. Fog detection

Fog events were detected using a Present Weather Sensor (PWS100, Campbell Scientific Inc., Logan, UT, United States), which is a laser-based sensor capable of determining atmospheric visibility. Its visibility ranges from 0 m to a maximum saturating distance of 20,000 m. The data were recorded every minute by a CR1000 data logger (Campbell Scientific Inc., Logan, UT, United States). Following the National Oceanic and Atmospheric Administration (1995), fog events are defined as occasions when visibility is < 1,000 m, and mist or light fog event as occasions when visibility is between 1,000 and 2,000 m (Vautard et al., 2009). Dense fog occurs when visibility is < 400 m (Witiw and LaDochy, 2008). The identification of fog events was first introduced by Tardif and Rasmussen (2007), and fog events are defined as occasions during which atmospheric visibility of < 2,000 m is recorded for at least 3 h within 5

sequential h, with a visibility of < 1,000 m recorded at least once in this time period. Thus, occasions with visibilities < 2,000 m lasting<2 h were not included in our study as fog events.

We compared the visibility data with precipitation data to distinguish rainfall from fog events. We excluded occasions when visibility was < 2,000 m with rainfall > 0.5 mm h^{-1} as well as occasions when visibility was < 1,000 m while rainfall was > 0.1 mm h^{-1}. It is noted that fog events occurred mostly during the dry season when rainfall is relatively scarce (Liu et al., 2004).

2.3. Eddy covariance flux and meteorological data

An open-path eddy covariance (EC) system comprising of an open-path infrared gas analyzer (Li-7500, Li-Cor Inc., Lincoln, NE, United States) with three-dimensional sonic anemometer (CSAT3, Campbell Scientific Inc., Logan, UT, United States) was installed at a height of 38 m on a 55 m triangular meteorological observation tower (Fig. S2). Seven levels of sensors (at 2.2, 8.7, 16.8, 21.3, 28.9, 37.8 and 56.6 m) were installed on the tower to obtain profiles of wind speed (WS) (A100R, Vector Instruments, Denbighshire, United Kingdom), Tair and RH (HMP45C, Vaisala, Helsinki, Finland). Instruments for measuring wind direction (WD) (W200P, Vector Instruments, Denbighshire, United Kingdom) and rainfall (P) (Rain Gauge 52203, R. M. Young Co., Traverse City, MI, United States) were mounted at the top of the tower. Rn was calculated from the downward and upward (short- and long-wave) radiations (CNR-1/CM11, Kipp and Zonen, Delft, the Netherlands) measured at a height of 28.6 m. PAR was monitored by line quantum sensors (LQS70-10, APOGEE, United States) at heights of 1.9 and 28.6 m. SM and soil temperature (Tsoil) profiles at depth of 5 cm, 20 cm and 100 cm were also recorded (CS616-L and 105/107 L, Campbell Scientific Inc., Logan, UT, United States, respectively). Two soil heat-flux plates (HFP01, Hukseflux, Netherlands) were used to monitor the average soil heat-flux. We also measured the leaf area index (LAI, m^2 m^{-2}) (Plant Canopy Analyzer-LAI-2000, Li-Cor Inc., Lincoln, NE, United States) and DBH (cm) twice per month. Leaf wetness was monitored using a resistance-based sensor (237-L, Campbell Scientific Inc., Logan, UT, United States) installed at a height of 7.8 m within the canopy. The wet–dry transition occurred at about 0.15 MΩ (i.e., a leaf with wetness < 0.15 MΩ is considered as wet). EC and meteorological data were separately logged using a CR5000 datalogger (Campbell Scientific Inc., Logan, UT, United States) at a frequency of 10 Hz and a CR1000 datalogger (Campbell Scientific Inc., Logan, UT, United States) every 30 min, respectively. To indicate the atmospheric water status, we calculated the atmospheric water potential (Ψatm, MPa) using Tair and RH following Vasey et al. (2012). The Ψatm was calculated as follows:

$$\Psi\mathrm{atm} = \left[\frac{R\cdot \mathrm{Tair}}{\partial \mathrm{Vw}}\right].\left[\ln\frac{RH}{100}\right] \quad (1)$$

where R is the universal gas constant, Tair is the air temperature (K), ∂V_w is the partial molal volume of water (cm^3/mol) and RH is the relative humidity.

2.4. CO_2 flux calculation

The NEE was calculated as follows (Aubinet et al., 1999; Baldocchi et al., 1996; Burba, 2013):

$$\mathrm{NEE} = \mathrm{Fc} + \mathrm{Fs} = \overline{\rho_d \omega' s'} + \frac{\Delta c}{\Delta t} Zr, \quad (2)$$

where Fc represents the turbulent eddy flux that is transported above the EC flux monitoring sensors height (38 m) and the atmosphere, Fs indicates the storage flux under the EC flux sensors and ground surface, ρ_d is the mean air density, ω is the vertical wind velocity and s the dry mole fractions. The primes denote deviations from the mean, and the overbar indicates a time average. The Δc is the discrete dynamic of CO_2 concentration over 30 min at 38 m height and Δt is the period of 30 min. A single point EC method was employed to compute Fs at the measurement height (zr) of the fluxes. Following the meteorological convention, negative NEE values indicate CO_2 uptake by the ecosystem and positive flux denotes CO_2 release into the atmosphere.

We used standard methodologies from FLUXNET and ChinaFLUX to process the raw data and control data quality (Reichstein et al., 2005; Yu et al., 2006). Specifically, three-dimensional coordinate rotation was applied to remove the effects of instrument tilt or irregularities in the terrain (Tanner and Thurtell, 1969; Wilczak et al., 2001). The Webb-Pearman-Leuning (WPL) correction was applied to correct for air density variations arising from the transfer of heat and water vapor (Webb et al., 1980). Storage flux corrections and hard spike exclusion were also performed (Sabbatini et al., 2018). Flux data recorded during intense rain events were eliminated (Yu et al., 2006). The outliers (NEE values > 50 or <−50 μmol $m^{-2}s^{-1}$) were identified and rejected (Reichstein et al., 2005). Negative nighttime NEE data were rejected if PAR was < 5 μmol $m^{-2}s^{-1}$ (Wang et al., 2013). The flux data with friction velocities (u^*) < 0.2 were filtered (Falge et al., 2001; Saleska et al., 2003; Reichstein et al., 2005). The surface energy balance showed a closure of 72% for the 30-min fluxes in the rubber plantations (Fig. S3). The average footprint (90%) reaches a radius of 244 m from the tower (Fig. S4). Finally, NEE values were gap filled using the marginal distribution sampling approach (Reichstein et al., 2005) and partitioned into GPP and ecosystem respiration (ER) using an online tool maintained by the Max Planck Institute, Jena, Germany (Wutzler et al., 2018). All the data processing methods were detailed in the earlier work of Fei et al. (2018).

In our study, WP_c (gC/kg H_2O) was defined as the ratio of GPP or yield to ET_c (Molden, 1997; Kijne et al., 2003; Zhou et al., 2015; and Fernández et al., 2020). Canopy conductance (Gs, mms^{-1}), which shows the efficiency of water exchange between the surface of ecosystem vegetation and the atmosphere, was estimated following empirical formulation by Noormets et al. (2010).

$$\mathrm{Gs} = \frac{pET_cR_w}{\rho_a \mathrm{VPD} R_d} \quad (3)$$

where p is atmospheric pressure (kPa), ET_c is crop evapotranspiration derived from EC ($kgm^{-2}s^{-1}$), R_w is universal gas constant specific for water vapor (461.495 J $kg^{-1}K^{-1}$), ρ_a is air density (kgm^{-3}), VPD is vapor pressure deficit (kPa) and R_d is universal gas constant specific for dry air (287.058 J $kg^{-1}K^{-1}$). Following Ewers and Oren (2000), Gs values were excluded in data analysis when VPD was ≤ 0.6 kPa.

2.5. Measurement of sap flow density

Around the EC flux tower, we randomly selected six rubber trees to measure the sap flow rate (Js) using the heat dissipation method following Granier (1985, 1987) (Fig. S2). Each sap flow probe setup consisted of two cylindrical metal needle probes (length: 20 mm; diameter: 2 mm). Sap flow probes were inserted radially into the outermost 2 cm of the stem at breast height (1.4 m) with a distance of approximately 10 cm between the two sensor probes to avoid thermal interference (Lin et al., 2018b). The probes of each unit were sealed with insulating silicone, and the whole system was covered with an aluminum reflector to protect it from solar radiation. Temperature differences between the upper (0.2 W) and lower probes (not heated), ΔT (°C), were measured and stored as 30-min averages using a data logger (CR10X, Campbell Sci., United States). Js ($gm^{-2}s^{-1}$) was calculated according to the Granier (1985) empirical equation:

$$\mathrm{Js} = \alpha\left(\frac{\Delta T\max}{\Delta T} - 1\right)^{\beta} \quad (4)$$

where ΔTmax indicates the temperature difference for zero sap flow, approximated by the maximum ΔT during nighttime. Uncertainty may arise while calculating ΔTmax from predawn ΔT values, because sap flow may continue even during the nighttime (Regalado and Ritter,

2007). However, the nighttime sap flow is expected to be small (Ludwig et al., 2006), especially under low VPD in FG days (Dawson et al., 2007). The empirical parameter α was 119 g $m^{-2}s^{-1}$, and the dimensionless parameter β was set to 1.231, according to Granier (1985).

Js was summed for each day to compute J_{out} in kg m^{-2} d^{-1}. Following Isarangkool Na Ayutthaya et al. (2011), the transpiration (T_c, mm d^{-1}) is computed from average J_{out} of six trees as:

$$T_c = 0.874 \times J_{out} \times \frac{s\_area}{t\_area} \quad (5)$$

where s_area and t_area are the sapwood area and tree-spacing area of the ecosystem, respectively. In this study, we used the s_area (0.04 m^2) and t_area (28.9 m^2) estimates from the same site by Zhao et al. (2014).

2.6. Statistical analysis

The turbulence regime is normally well developed between 06:00 and 21:00 in hilly regions (Mildenberger et al., 2009). Since this study mainly focuses on processes that occur during the daytime (i.e., ecosystem CO_2 uptake and WP_c), only data between 06:00 and 21:00 were used. Given that ecosystem respiration were not significantly different between FG and non-FG days during both the cool and hot dry seasons (Fig. S5), excluding nighttime data does not affect our comparison of CO_2 fluxes between FG and non-FG days. The daily mean values of physiological (NEE, GPP, ET_c, WP_c, Gs and T_c) and micrometeorological (Tair, VPD and PAR) variables were computed and compared between the FG and non-FG days during the cool and hot dry seasons. We performed one-way analysis of variance (ANOVA) to test the differences (alpha = 0.05) in ecosystem physiological responses and meteorological variables between FG and non-FG days only during the dry season, followed by the Tukey's test using the 'emmeans' R package (Lenth et al., 2021). The monthly differences between P and ET_c (P-ET_c) were calculated to indicate the water deficit conditions of the rubber plantations during the entire study period. A multiple linear model was used to evaluate the physiological responses to the changes of the meteorological variables. Dominance analysis was carried out to determine the contribution of each predictor using the 'dominance analysis' R package (Navarrete, 2020). Further analyses included linear regressions to evaluate the relationships between ecosystem carbon/water fluxes (i.e., NEE, GPP, ET_c, WP_c, T_c and Gs) and micrometeorological variables (Tair and VPD) in cool dry FG and non-FG days. These analyses were performed using the 'lm' function in R (Version 3.6.0, R core Team 2019). Graphs were made using the R package 'ggplot2' (Wickham, 2016).

3. Results

3.1. Meteorological parameters and fog occurrences

The mean monthly Tair was 22.3 ± 3.7 °C, with values ranging from 6.6 °C (January 2016) to 31.5 °C (May 2014) (Fig. 1). The Tsoil at 5 cm was higher during the dry season than during the wet season. The highest (38.7%, 2015) and lowest (8.5%, 2014) SM values at a depth of 5 cm were observed during the wet season and dry season, respectively. Similarly, the SM at 100 cm was higher during the wet season than

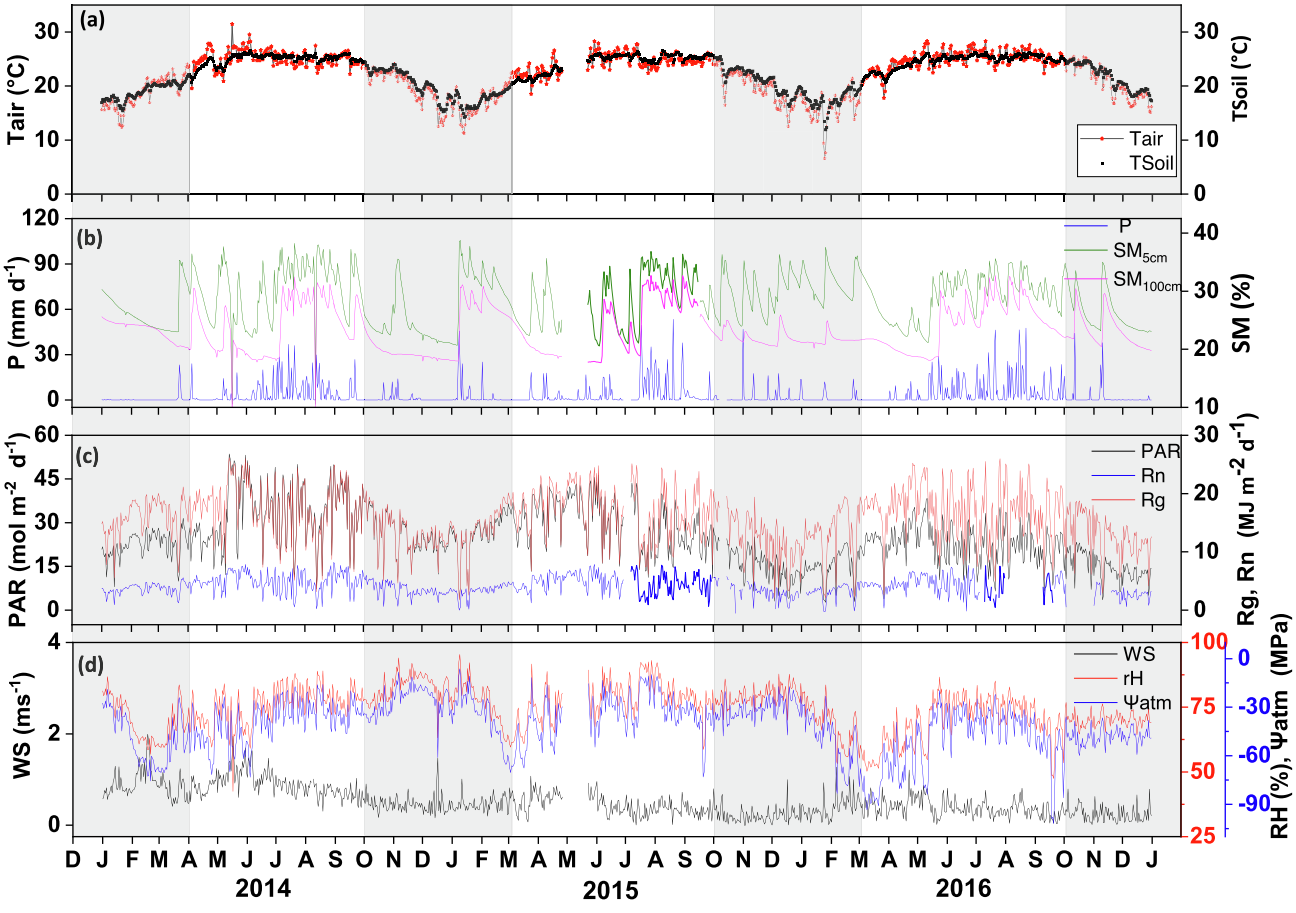

Fig. 1. Continuous daily averaged meteorological data from 2014 to 2016 of (a) air temperature (Tair), soil temperature (Tsoil at depth of 5 cm); (b) precipitation (P), soil moisture content (SM) at depths of 5 cm (SM_{5cm}) and 100 cm (SM_{100cm}); (c) photosynthetically active radiation (PAR), global radiation (Rg) and net radiation (Rn); (d) wind speed (WS), relative humidity (RH) and atmospheric water potential (Ψatm). The gray vertical columns in each panel represent the dry period across the cool dry and hot dry seasons, and the white areas characterize the wet season.

during the dry season. The annual P during the study period (January 2014–December 2016) was 1,149 mm at the site and the mean global solar radiation (Rg), Rn and PAR at the site were 15.45 ± 4.8 MJ m^{-2} d^{-1}, 8.2 ± 3.3 MJ m^{-2} d^{-1} and 24.86 ± 9 mol m^{-2} d^{-1}, respectively. The mean monthly RH was 71 ± 10%, the mean annual WS was 0.5 m s^{-1} and the frequency of calm days was about 75%. The mean monthly Ψatm was −41.1 ± 15.2 MPa, with values ranging from −102 MPa (September 2016) to −6.2 MPa (January 2015) (Fig. 1).

A total of 423 fog events were identified over the 3-year study period. The year 2016 experienced the most fog events (150), whereas the lowest number of events (128) was recorded in 2015 (Fig. 2a). Season-wise, 75.7% of the total events occurred during the dry season and 24.3% during the wet season (Table S1). January is the most fog-prone month (17%), whereas June is the least (1.3%). The mean duration of fog events is 3.2 ± 2.8 (SE) h, while 55% of the fog events lasted for 2–5 h (Fig. 2b). On average over 2014–2016, the longest fog events were 8.3 ± 6.7, 5.2 ± 0.7, 4.1 ± 1.1 and 4.5 ± 3.3 h/day for December, January, February and March, respectively. About 72% of P occurred during the wet season of the study period (Fig. 2c). During the fog events, the minimum atmospheric visibility was within 100–400 m (dense fog), 500–800 m and 900–1,000 m in 44%, 25% and 31% occasions, respectively (Fig. 3a). Fog occurred mostly in the early morning hours (02:00–10:00) and dissipated 1–2 h after sunrise (Fig. 3b). The leaf-wetting (i.e., leaf wetness drops below 0.15 MΩ) events due to fog were also frequent in the early morning hours, and dry seasonal canopy wet conditions lasted on average for 8.8 h/day in FG days (Fig. 3c).

3.2. Changes in micrometeorological factors on foggy days

Compared with non-FG days in the cool dry season, we observed an 5% ($p < 0.01$) reduction in Tair on cool dry FG days. Particularly in the months of December and January, the average Tair was 16 °C and 16.5 °C on cool dry FG and non-FG days, respectively (Fig. 4a). Whereas, average Tair was found to be similar level during the FG (22.6 °C) and non-FG (22.7 °C) days of hot dry season. Further, we observed no significant changes in VPD, Ψatm and RH on FG days relative to non-FG days in both cool and hot dry seasons (Fig. 4 b,c,e). A 192% ($p < 0.01$) increases in leaf wetness were found on FG days when compared with non-FG days of both cool and hot dry seasons (Fig. 4d). We found 17% increases in daytime PAR ($p < 0.01$) on FG days relative to non-FG days of cool dry season, however same level of PAR was noticed during the hot dry season of FG and non-FG days. (Fig. 4f).

3.3. Physiological effects of fog on rubber plantations

The NEE, GPP, ET_c, WP_c, Gs and T_c were generally higher in the wet season than during the dry season (Fig. 5a–f). In the middle of February, during the dry season, there was a brief but sharp drop in GPP and WP_c due to leaf shedding of the rubber tree, which recovered after new leaves began to sprout in March. The NEE (cool dry, $p = 0.47$ and hot dry, $p = 0.99$), GPP (cool dry, $p = 0.93$ and hot dry, $p = 0.78$) and T_c (cool dry, $p = 0.77$ and hot dry, $p = 0.47$) showed no significant differences between FG and non-FG days in both cool and hot dry seasons (Fig. 6). The ET_c and Gs reduced by 15%, and 38%, respectively, in FG days relative to non-FG days in the cool dry season ($p < 0.01$), but they were not different between the FG and non-FG days in the hot dry season. Interestingly, WP_c increased significantly by 12.3% during cool FG compared with cool non-FG days ($p < 0.01$) but insignificant during hot FG and hot non-FG days.

We found that for most of the dry season (except January 2015), P-ET_c was < 0 mm, which indicates water deficit (Fig. 7a). The SM in the top soil layer (5 cm) showed distinct seasonal variations with the values

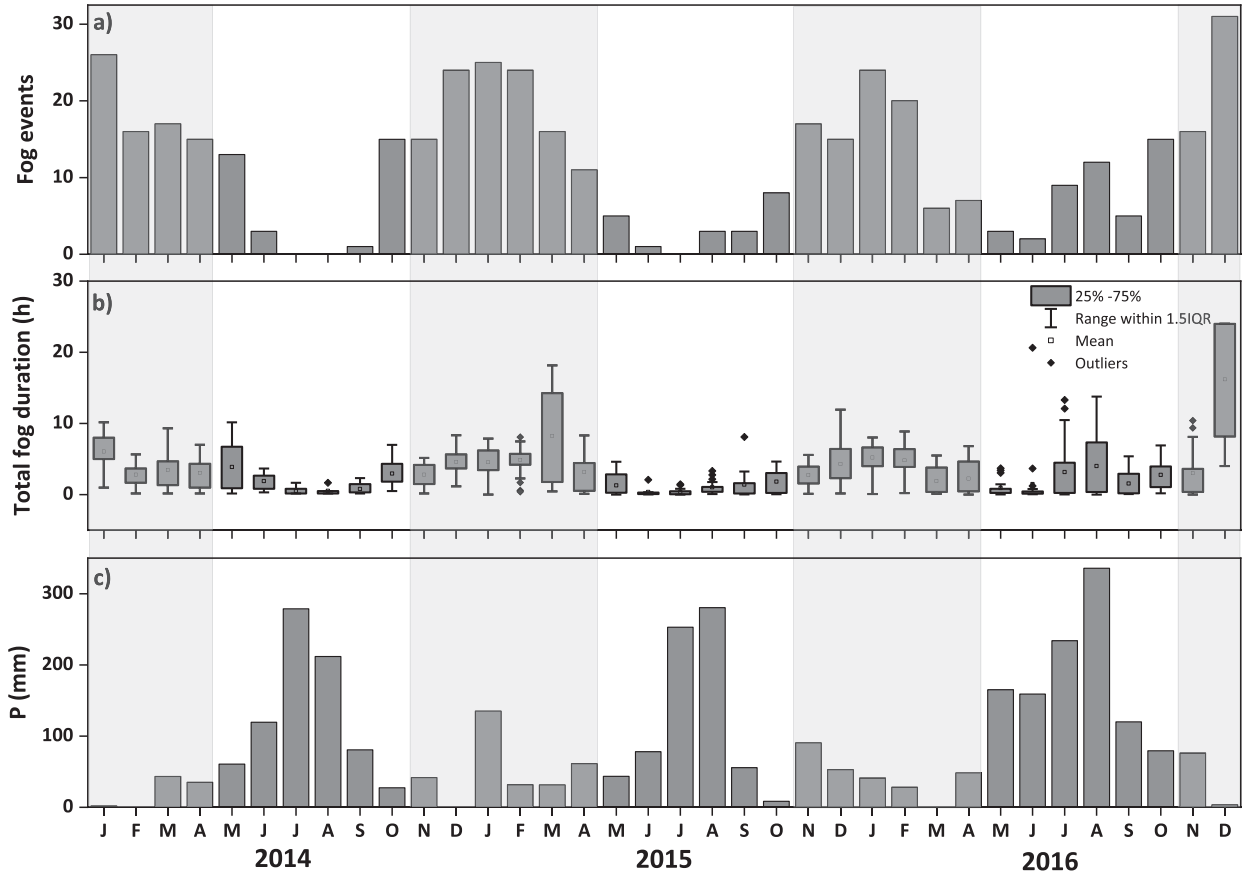

Fig. 2. Monthly number of fog events (a), total durations (h) of the fog events (b), and rainfall (P, mm) (c) during 2014–2016 at the study site. Gray backgrounds represent the dry seasons.

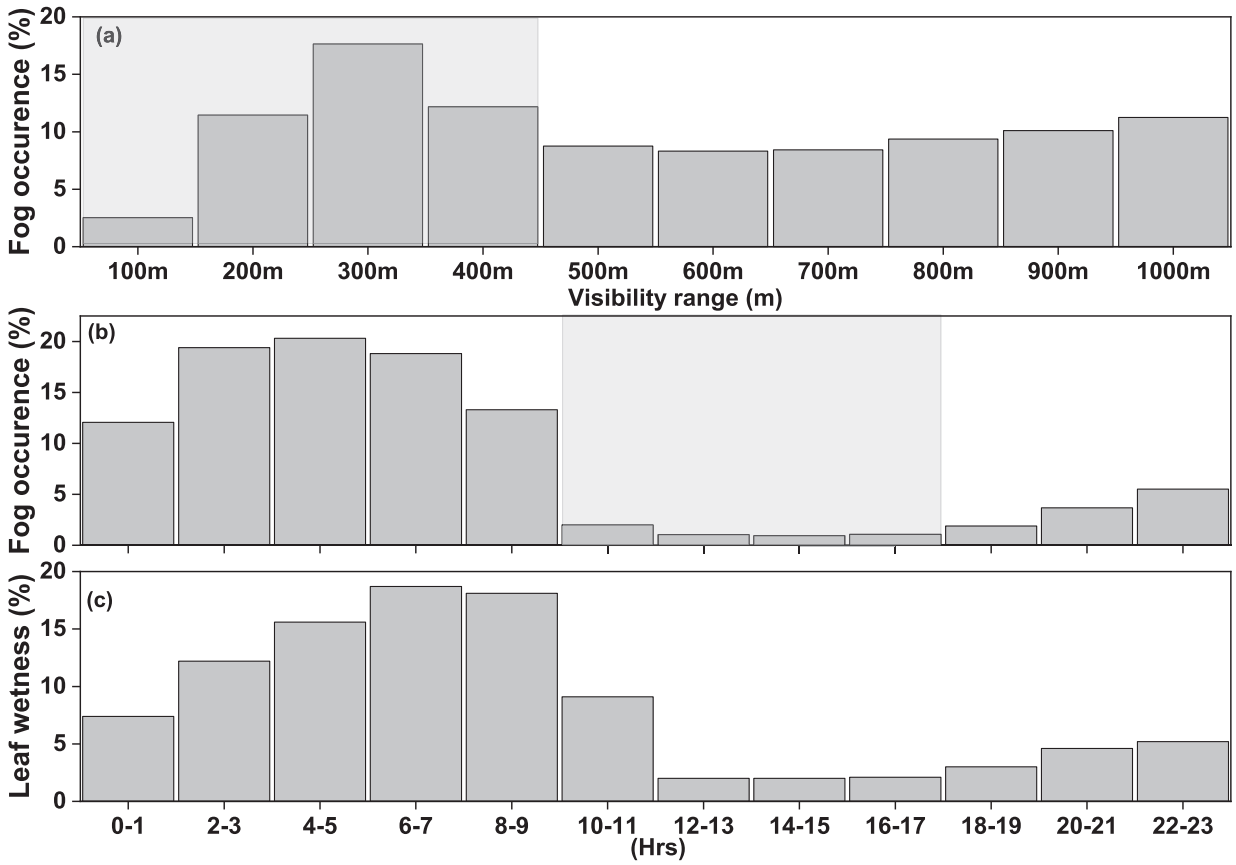

Fig. 3. (a) Minimum visibility distribution frequencies compiled for the totality of fog occurrence for the 2014–2016 period (gray color mark indicates the dense fog days, <400 m visibility); (b) total fog frequency distribution in a day on an hourly basis (gray color mark indicates the dissipation time of fog); (c) total leaf wetness frequency distribution in a day on an hourly basis for the 2014–2016 dry season only. (Due to a lack of continuous leaf wetness measurements in the rubber plantation site, the data was obtained from a tropical rainforest site, which is 5 km away in the same region.).

ranging from 22% (December 2014) to 34% (August 2014), and the values were generally lower during the dry season (27.7 ± 3%) than during the wet season (29.4 ± 2.8%) (Fig. 7b). Overall, the ecosystem was exposed to soil water stress from the beginning of October to the end of April.

3.4. Dependence of physiology on meteorological variables

Multiple linear regression models explained 40%, 48%, 30%, 26%, 53% and 41% of the NEE, GPP, ET_c, WP_c, Gs and T_c variances, respectively, during cool dry FG days (Table 1). The VPD ($p < 0.001$) was the most important factor in explaining the NEE (60%), GPP (75%) and WP_c (60%) models, while Tair had the highest contributions in the ET_c (86%), Gs (44%) and T_c (62%) models for cool dry FG days. Similar to cool dry FG days, the models for the cool dry non-FG days also explained 35%, 33%, 33%, 12%, 54% and 10% of the variances for NEE, GPP, ET_c, WP_c, Gs and T_c, respectively. Similar to cool dry FG days, VPD ($p < 0.001$) also had significant contribution in the NEE (52%), GPP (51%), and WP_c (55%) models, while Tair had the highest contributions in the ET_c (71%), Gs (64%) and T_c (94%) models on cool dry non-FG days. Finally, on both cool dry FG and non-FG days, Tair and VPD were the significant factors in most models (Table 1).

The VPD ($p < 0.001$) was the most important factor in explaining the NEE (60%), GPP (58%) and WP_c (73%) models, while Tair had the highest contributions in the ET_c (86%), and T_c (62%) models for hot dry FG days. The PAR had the highest influences in the Gs (65%) models for hot dry FG days. In contrast with hot dry FG days, Tair ($p < 0.001$) had significant contribution in the NEE (84%), GPP (89%), WP_c (41%) and T_c (91%) models, while PAR and VPD had the highest contributions in the ET_c (44%) and Gs (76%), respectively in hot dry non-FG days. Finally, we were not found any similar kind of most significant factors in both hot dry FG and non-FG days (Table.1).

On both cool dry FG and non-FG days, the NEE increased linearly with VPD (slope: 0.69, $R^2 = 0.30$, $p < 0.001$, and slope: 0.36, $R^2 = 0.14$, $p < 0.001$), respectively (Fig. 8a), however cool dry FG days showed higher positive relationship than the cool dry non-FG days. The GPP generally decreased with increasing VPD (slope: −0.77, $R^2 = 0.40$, $p < 0.001$) on cool dry FG days, but on the cool dry non-FG days relationships were significantly lower than the cool dry FG days (VPD: slope: −0.42, $R^2 < 0.15$, $p < 0.001$) (Fig. 8b). On both FG and non-FG days of cool dry season, WP_c decreased with increasing VPD (slope = -0.33, $R^2 = 0.22$, $p < 0.001$ and slope = -0.18, $R^2 = 0.1$, $p < 0.001$) (Fig. 8c), respectively. Further, a positive relationship was present between ET_c and Tair (slope = 0.13, $R^2 = 0.25$, $p < 0.001$) on FG days and also on non-FG days of cool dry season (slope = 0.13, $R^2 = 0.27$, $p < 0.001$) (Fig. 8d). T_c and Tair had a positive significant relationship (slope = 0.1, $R^2 = 0.23$, $p < 0.001$) on cool dry FG and non-FG days (slope = 0.05, $R^2 = 0.1$, $p = 0.003$) (Fig. 8e). Gs was positively correlated with Tair on both FG (slope: 0.76, $R^2 = 0.18$, $p < 0.001$) and non-FG days of cool dry season (slope: 0.86, $R^2 = 0.27$, $p < 0.001$) (Fig. 8f).

4. Discussion

4.1. Variations in fog occurrence

Seasonal fog is a common phenomenon in montane regions (Bruijnzeel et al., 2011). To monitor fog events with higher accuracy, laser-based sensor is an important first step in understanding how fog

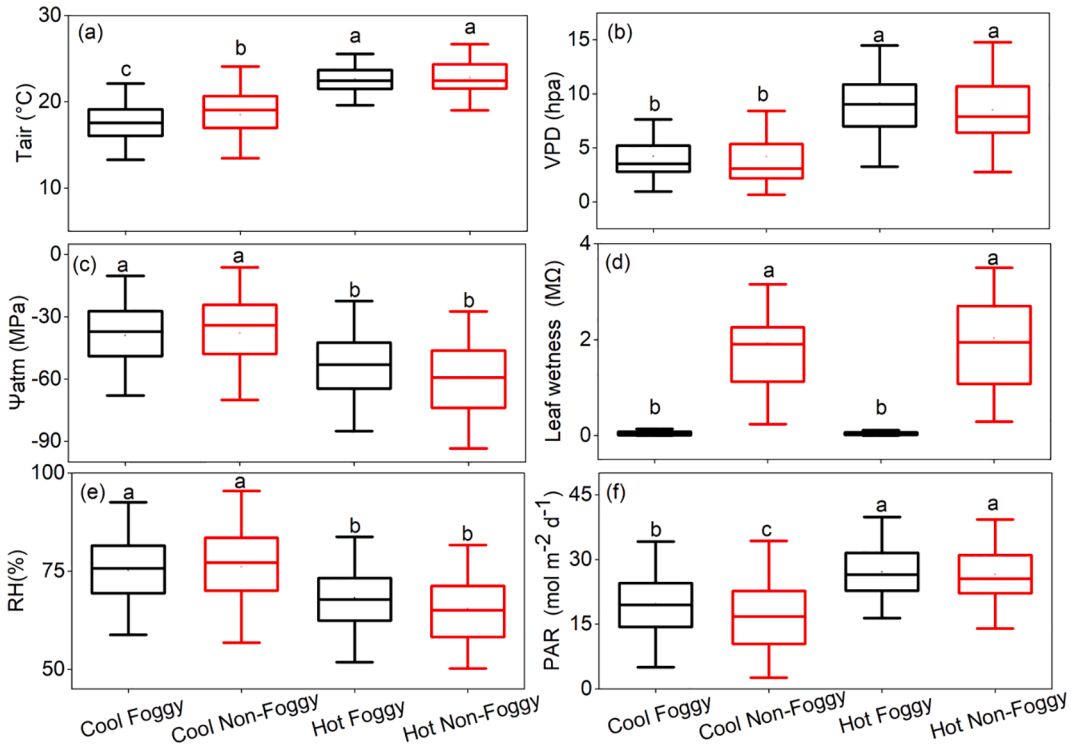

Fig. 4. Differences in micrometeorological variables between foggy and non-foggy days in the cool and hot dry seasons over 2014–2016. These variables include (a) air temperature (Tair), (b) vapor pressure deficit (VPD), (c) atmospheric water potential (Ψatm), (d) leaf wetness, (e) relative humidity (RH) and (f) photosynthetically active radiation (PAR). For each boxplot, the horizontal line within the box indicates the median. The lower and upper edges of the box are the 25th and 75th percentiles, respectively. The upper and lower whiskers are min/max values. Differences were determined using the Tukey's test and the significant differences between cool and hot dry foggy and non-foggy days are shown by different letters ($p < 0.01$). Boxes containing the same letter are not significantly different ($p > 0.05$).

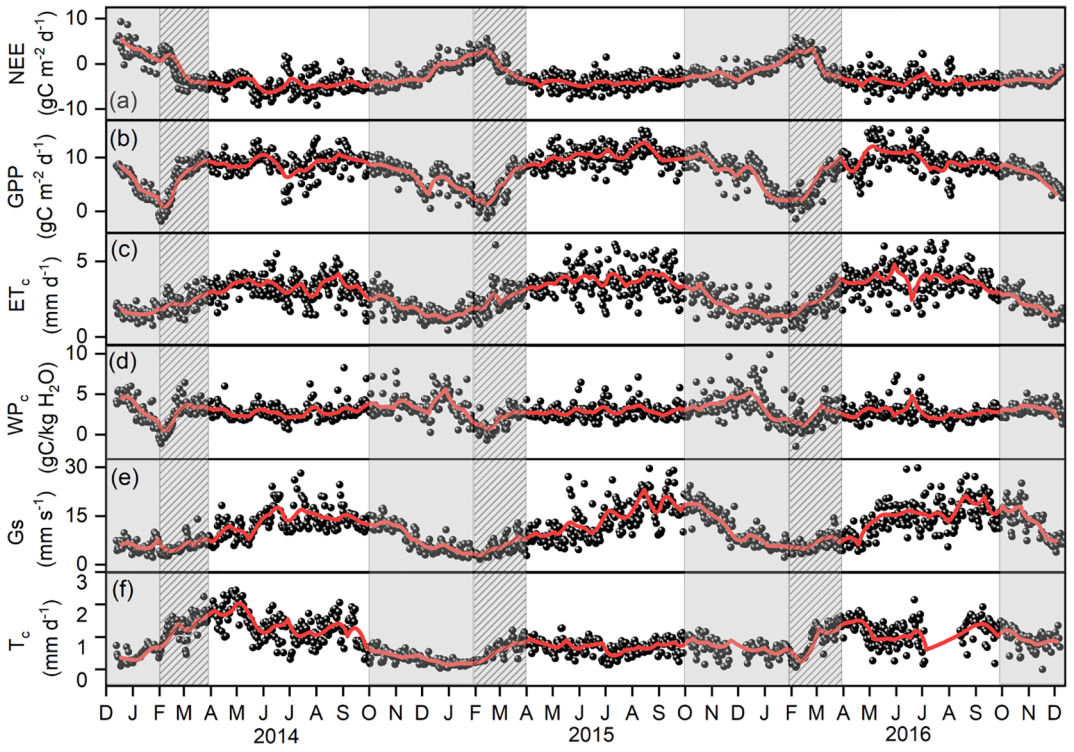

Fig. 5. (a) Daily average net ecosystem exchange (NEE), (b) gross primary production (GPP), (c) evapotranspiration (ET_c), (d) crop water productivity (WP_c), (e) canopy conductance (Gs) and (f) tree transpiration (T_c) from 2014 to 2016. Red lines indicate the weekly moving average values. Clean and crossed gray backgrounds represent the cool dry and hot dry seasons, respectively. (For interpretation of the references to color in this figure legend, the reader is referred to the web version of this article.)

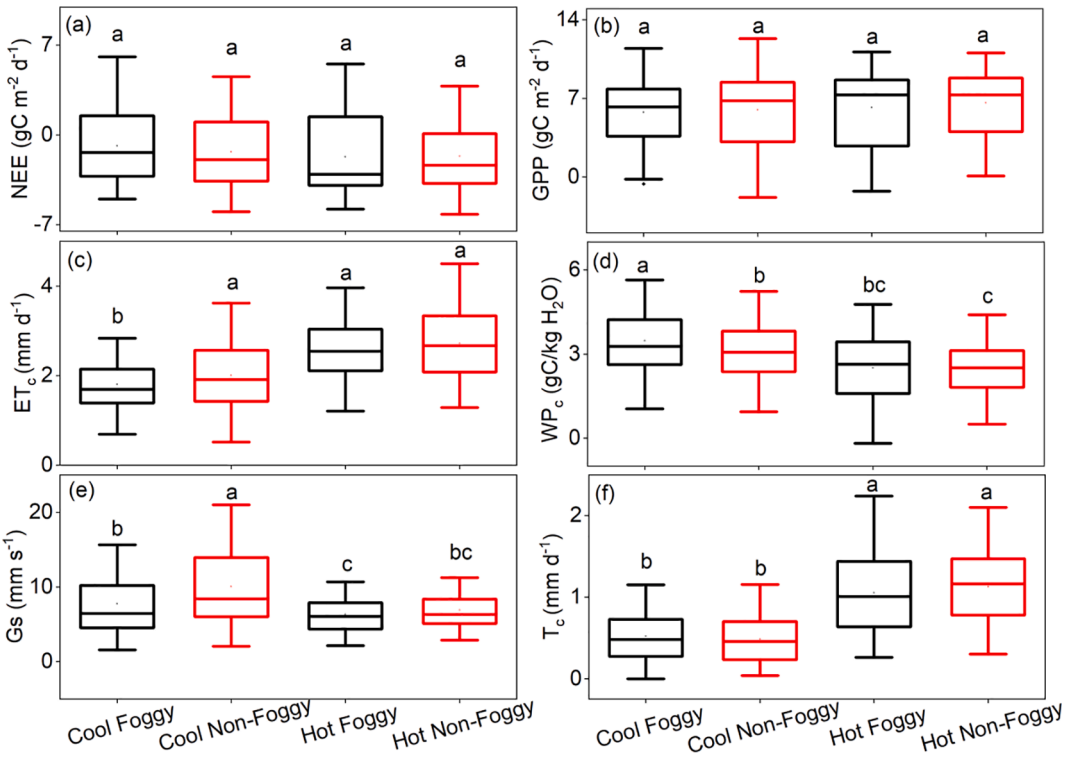

Fig. 6. Differences in dry seasonal average values of (a) net ecosystem exchange (NEE), (b) gross primary production (GPP), (c) crop evapotranspiration (ET_c), (d) crop water productivity (WP_c), (e) canopy conductance (Gs) and (f) tree transpiration rate (T_c) between cool and hot dry foggy (black) and cool and hot dry non-foggy (red) days at the rubber plantations for the record spanning the period starting from 2014 to 2016. For each boxplot, the horizontal line within the box indicates the median. The lower and upper edges of the box are the 25th and 75th percentiles, respectively. The upper and lower whiskers are min/max values. Differences were determined using the Tukey's test, and the significant differences between cool and hot dry foggy and non-foggy days are shown by different letters ($p < 0.01$). Boxes containing the same letter are not significantly different ($p > 0.05$). (For interpretation of the references to color in this figure legend, the reader is referred to the web version of this article.)

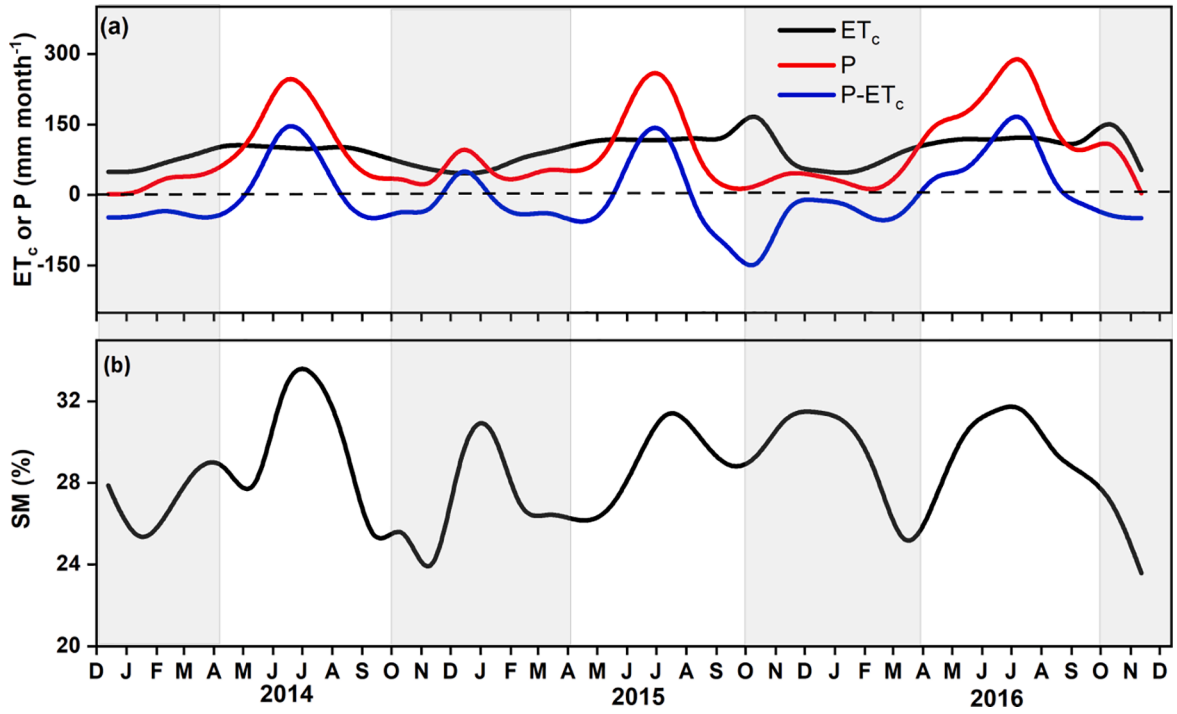

Fig. 7. (a) Variations of monthly crop evapotranspiration (ET_c), precipitation (P) and their differences ($P\text{-}ET_c$); and (b) soil moisture (SM) at a depth of 5 cm from 2014 to 2016. Gray backgrounds represent the dry season.

Table 1
The summary of multiple linear regression models for NEE, GPP, ET_c, WP_c, Gs and T_c for foggy and non-foggy days during the cool and hot dry seasons.

		Cool Dry Foggy				Cool Dry Non-Foggy				Hot Dry Foggy				Hot Dry Non-Foggy			
Model	Predictor	Coeff (SE)	t-value	Contribution	R^2	Coeff (SE)	t-value	Contribution	R^2	Coeff (SE)	t-value	Contribution	R^2	Coeff (SE)	t-value	Contribution	R^2
NEE	Intercept	2.43 (1.04)	2.33 *	–	0.4	4.2 (1.35)	3.1 **	–	0.35	8.1 (4.2)	2	–	0.4	10.3 (3)	3.63 ***	–	0.14
	Tair	−0.35 (0.05)	−6.31 ***	22%		−0.35 (0.1)	−4.44 ***	41%		−0.7 (0.2)	−4 ***	34%		−0.5 (0.1)	−3.88 ***	84%	
	VPD	0.75 (0.1)	8.43 ***	60%		0.52 (0.1)	5.8 ***	52%		0.45 (0.1)	5 ***	62%		0.1 (0.1)	1.1	5%	
	PAR	−0.01 (0.03)	−0.36	18%		−0.1 (0.03)	−1.8 *	7%		0.04 (0.04)	1.1	4%		−0.04 (0.04)	−1	11%	
GPP	Intercept	3.71 (0.92)	4 ***	–	0.48	−0.13 (1.5)	−0.1	–	0.33	−7 (4.1)	−1.72	–	0.5	−9.55 (2.72)	−3.5 ***	–	0.25
	Tair	0.26 (0.05)	5.24 ***	10%		0.43 (0.1)	4.8 ***	45%		1 (0.2)	5 ***	38%		0.73 (0.12)	5.75 ***	89%	
	VPD	−0.96 (0.08)	−12.04 ***	75%		−0.52 (0.1)	−5.14 ***	51%		−0.54 (0.1)	−6 ***	58%		−0.18 (0.1)	−2 *	6%	
	PAR	0.07 (0.02)	2.86 **	15%		0.02 (0.04)	0.5	4%		−0.05 (0.04)	−1.2	4%		0.03 (0.04)	1	5%	
ET_c	Intercept	−0.47 (0.26)	−1.84 *	–	0.3	−0.2 (0.4)	−0.53	–	0.33	−2.6 (1.1)	−2.33 *	–	0.25	−1 (0.7)	−1.23	–	0.4
	Tair	0.13 (0.01)	9.41 ***	86%		0.11 (0.02)	5.5 ***	71%		0.22 (0.05)	4.5 ***	92%		0.08 (0.03)	2.65 **	25%	
	VPD	−0.1 (0.02)	−3.9***	11%		−0.1 (0.02)	−3.24 **	14%		−0.003 (0.02)	−0.13	1%		0.05 (0.02)	2.36 *	31%	
	PAR	0.02 (0.01)	2.4 *	3%		0.02 (0.01)	2 *	15%		0.01 (0.01)	1	7%		0.04 (0.01)	3.78 ***	44%	
WP_c	Intercept	6.9 (0.63)	11 ***	–	0.26	4.7 (1)	5 ***	–	0.12	4.1 (2)	2.17 *	–	0.4	0.1 (1.18)	0.1	–	0.13
	Tair	−0.11 (0.03)	−3.41 ***	17%		−0.03 (0.05)	−0.54	9%		0.1 (0.1)	1.1	2%		0.17 (0.05)	3.14 **	41%	
	VPD	−0.31 (0.05)	−5.58 ***	60%		−0.13 (0.1)	−2.1 *	55%		−0.22 (0.04)	−5.2 ***	73%		−0.1 (0.04)	−2.3 *	32%	
	PAR	−0.004 (0.02)	−0.25	23%		−0.03 (0.02)	−1.1	36%		−0.05 (0.02)	−2.6 **	25%		−0.02 (0.01)	−1.63	27%	
Gs	Intercept	−2.25 (1.44)	−1.56	–	0.53	−5.5 (2)	−3 **	–	0.54	7.4 (4)	1.86 *	–	0.25	7.32 (2.71)	2.7 **	–	0.01
	Tair	0.9 (0.07)	11.2 ***	44%		1.14 (0.11)	10 ***	64%		0.21 (0.17)	1.26	5%		0.01 (0.12)	0.15	14%	
	VPD	−1.13 (0.12)	−9.1 ***	41%		−0.65 (0.13)	−5 ***	27%		−0.2 (0.1)	−2.23 *	31%		−0.1 (0.1)	−1	76%	
	PAR	−0.03 (0.04)	−0.8	15%		−0.2 (0.05)	−3 **	9%		−0.15 (0.04)	−3.6 ***	64%		−0.01 (0.04)	−0.25	10%	
T_c	Intercept	−0.17 (0.12)	−1.44	–	0.41	0.1 (0.4)	0.2	–	0.1	−1 (0.67)	−1.4	–	0.3	−2 (0.35)	−5.5 ***	–	0.48
	Tair	0.06 (0.01)	9.81 ***	62%		0.05 (0.02)	2.4 *	94%		0.11 (0.02)	4.05 ***	60%		0.15 (0.01)	9.2 ***	91%	
	VPD	0.001 (0.01)	0.12	8%		−0.001 (0.02)	−0.04	1%		−0.04 (0.01)	−2.75 **	32%		−0.01 (0.01)	−1	5%	
	PAR	−0.02 (0.003)	−6 **	30%		−0.001 (0.01)	−0.12	5%		−0.01 (0.01)	−1.4	8%		−0.01 (0.005)	−2.06 *	4%	

ET_c: crop evapotranspiration (mmd^{-1}); GPP: gross primary production ($gCm^{-2}d^{-1}$); Gs: canopy conductance ($mm\ s^{-1}$); NEE: net ecosystem exchange ($gCm^{-2}d^{-1}$); PAR: photosynthetically active radiation ($molm^{-2}d^{-1}$); Tair: air temperature (°C); T_c: Tree transpiration (mmd^{-1}); VPD: vapor pressure deficit (hPa); WP_c: crop water productivity ($gC/kg\ H_2O$). *The coefficient is significant at $p < 0.05$; **The coefficient is significant at $p < 0.01$; ***The coefficient is significant at $p < 0.001$.

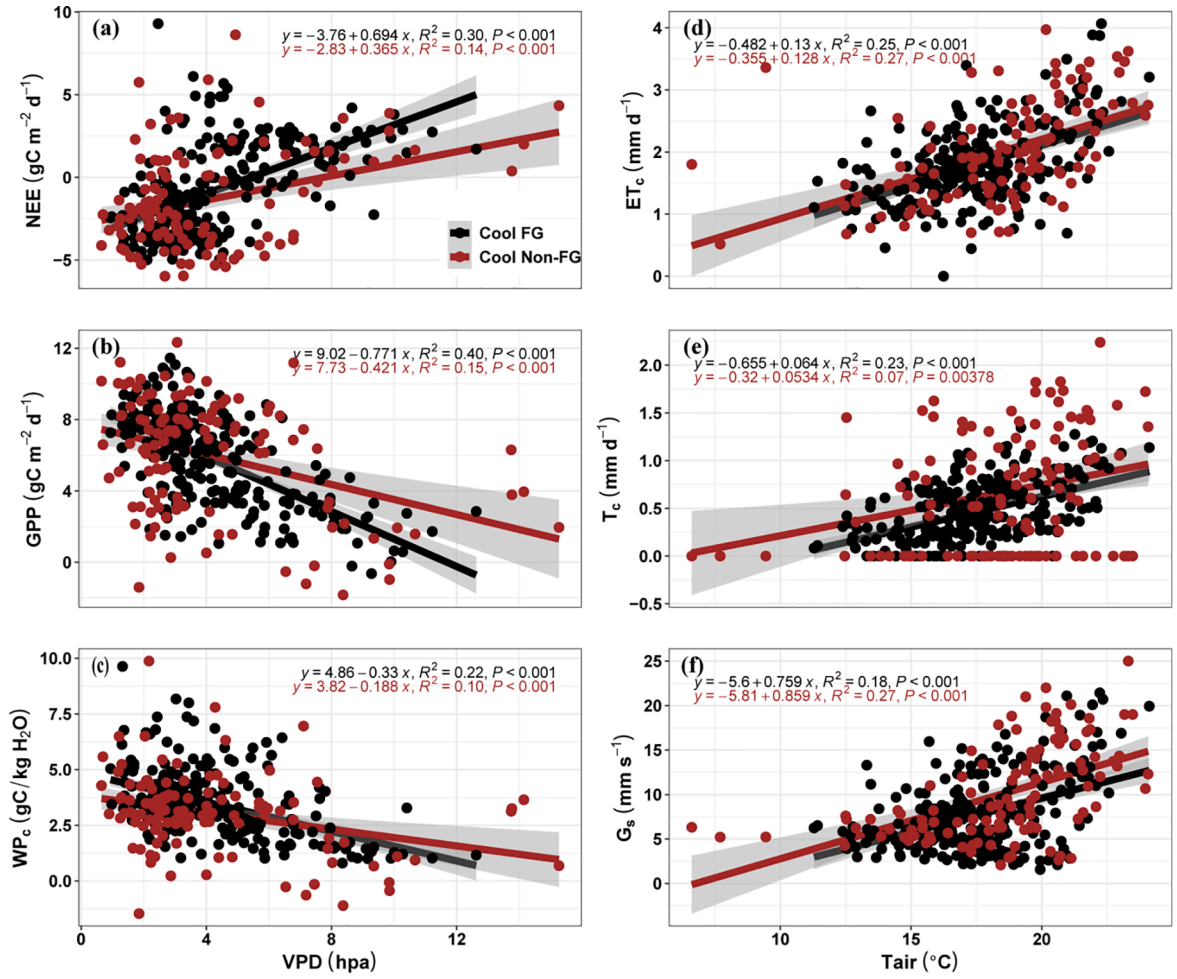

Fig. 8. Linear regression for daily net ecosystem exchange (NEE) (a), gross primary production (GPP) (b), crop water productivity (WP_c) (c), daily crop evapotranspiration (ET_c) (d), tree transpiration rate (T_c) (e) and canopy conductance (Gs) (f) as a function of the vapor pressure deficit (VPD) or air temperature (Tair) on cool dry foggy (cool FG) and cool dry non-foggy (cool non-FG) days of 2014–2016. The gray bands denote the 95% CI.

influences the tropical rubber tree's function. The fog occurrence in Xishuangbanna region was more frequent during the dry season than during the wet season (Table S1). The fog mainly forms around 3:00 a.m. and dissipates 1–2 h after sunrise in most fog events (80%) of the year (Figs. 2–3). However, our data (141 ± 12 fog events annually) indicates that fog events were much fewer than the earlier reported values (258 ± 58 fog events annually) (Liu et al., 2004), and this could be due to the large-scale deforestation of tropical rainforests and conversion into monoculture rubber plantations in Xishuangbanna in the past decade (Zhang et al., 2014). The rubber plantations have a lower LAI than tropical rainforest (Rusli and Majid, 2014). Thus, canopy alteration increases the albedo (higher radiation reflection ratio), which reduces the overall clouds/fog in the region (Hauser et al., 2015). Our results suggest that the highly frequent dense fog events were of the radiation fog type (Tardif and Rasmussen, 2007) and occurred in the cool dry season (November–February). The dense fog events reduce chilling damage to tropical plants, including rubber trees, and help maintain the tropical rainforests as well as agricultural crops of the region (Zongdao and Xueqin, 1983; Zhang et al., 2014).

4.2. Fog events enhance crop water productivity

We found significant improvement (12.3%) in ecosystem WP_c in FG days in the cool dry season even with the deciduous nature of rubber trees (intense leaf shedding from January to February; Fig. S6), but not in the hot dry season (Fig. 6). This enhanced WP_c was mainly induced by the reduction in ET_c while NEE and GPP showed no significant changes on cool dry FG days when compared with cool dry non-FG days. The difference in ET_c was mainly due to the decreased evaporation during cool dry FG days, whereas no significant changes of T_c was noticed as rubber trees are less active during this period due to leaf senescence. After the short, rubber trees started to actively transpire as new leaves grew in hot dry season, leading to no ET_c difference between FG and non-FG days (Fig. 6). The low evapotranspiration during fog events is associated with low VPD, which reduces atmospheric water stress (Ritter et al., 2009; Alvarado-Barrientos et al., 2014). The enhanced WP_c found on cool dry FG days in this study is consistent with other observations, for example, in a strawberry crop field (Baguskas et al., 2018, 2021). The water-stressed crops can also use dew as a water resource in semi-arid maize fields, resulting in greater WP_c (Yokoyama et al., 2021). In contrast to our study, the WP_c increase under FG conditions was driven by reductions in both ET_c and NEE with sharper drops in ET_c than in NEE (Gerlein-Safdi et al., 2018b; Baguskas et al., 2018), whereas we found no changes in NEE of the rubber plantation on cool dry FG days compared with cool dry non-FG days (Fig. 6). The dry season represents the driest period with little rainfall in Xishuangbanna. The net carbon uptake is the lowest during the cool dry season (Fig. 5), which could make the trees vulnerable to the drought stress. The foggy conditions in the cool dry season enhance ecosystem WP_c via evaporation reduction and decrease water loss from the system, which could be an important mechanism to mitigate the plant physiological stress and impairment in response to the drought during the period.

The high carbon uptake rates of the rubber plantation were mainly linked to the timing of the fog events, which can affect plant physiological functions (Bittencourt et al., 2019). In most studies, the fog events occur from morning to afternoon, which limits the transpiration and plant productivity (Ritter et al., 2009; Baguskas et al., 2018, 2021). At our site, most of the fog events (80%) lasted from midnight to early morning, and fog usually dissipated within 2 h of sunrise. Consequently, the canopy remained wet for ~ 8.8 h till mid-day (Fig. 3c), driving leaf water uptake and the rehydration of plant tissues, which resulted in the overall reduction of transpiration (Eller et al., 2013; Chu et al., 2014; Alvarado-Barrientos et al., 2015). At the same time, dissipated fog did not significantly affect the light availability on FG days (Fig. 4f). Consequently, rubber trees can still maintain a high carbon uptake rate on FG days. Considering the trade-off between water loss and carbon uptake, our study suggests that fog events help increase the efficiency of plant water use, which enhances the tolerance of rubber trees to drought stress during the dry season.

4.3. Foggy days suppress T_c and ET_c

We found insignificant changes in T_c over cool dry season are due to the intense defoliation and low temperature which suppressed the transpirations rate (January to February) (Fig. 6, S6), which is inconsistent with findings from other forests and crop fields with frequent fog occurrences. For example, tree transpiration was suppressed, which ranged from 25% to 40% under FG conditions when compared with non-FG conditions in various forest ecosystems (Hutley et al., 1997; Ritter et al., 2009; Gerlein-Safdi et al., 2018b). Similarly, several studies also highlighted that the presence of fog affects the microclimatic conditions and reduces evapotranspiration in tropical montane cloud forest ecosystems (Hildebrandt et al., 2007; Bruijnzeel et al., 2011; Bittencourt et al., 2019), potato farm (Ramírez et al., 2018) and also in a strawberry farm (Baguskas et al., 2021), which is consistent with our findings that ET_c (15%) rates (ecosystem water loss) were significantly suppressed during cool dry fog events (Fig. 6). Most of these studies suggest that the suppressed T_c and ET_c during fog events is likely related to the associated changes in Tair, VPD, Ψatm, lower radiation and frequent canopy wetting (Ritter et al., 2009; Baguskas et al., 2018). We also obtained evidence that the fog reduced the Tair and VPD, which were significantly ($p < 0.001$) correlated to T_c and ET_c in FG days (Table 1; Fig. 8). This could be due to lower Tair and VPD which lead to a reduced evaporative demand (Fig. 4) and lower the water stress during the dry season (Fig. 7). The fog events subsequently should enhance the leaf and stem water potential that reduces the water demand in the dry season, which was also evidenced from the study of Fu et al. (2016), who demonstrated that fog is an important water source for woody plants in the Asian tropical karst forest of Xishuangbanna. Thus, it is likely that rubber trees utilize fog as additional source of water through foliar water uptake during leaf wetting events (Eller et al., 2013, 2016; Berry et al., 2014). This pathway can be particularly important to alleviate drought stress during prolonged dry season (Elliott et al., 2006; Fu et al., 2016). At the same time, the increased Ψatm also facilitated rehydration for plants under conditions of soil water deficit (Baguskas et al., 2018). We suggest that leaf-wetting events, which enhance leaf surface vaporization and minimize T_c rates, can be a major driver for the ET_c for the rubber plantation and should be considered in future studies regarding tropical fog. Overall, frequent leaf wetting and reduced atmospheric water stress due to fog events could be important water sources for tropical crops, particularly in the dry season.

The magnitude of transpiration largely depends on soil water status as well as atmospheric water demand (Teuling and Troch, 2005). The sharp SM decrease in the dry season was due to the shortage of rainfall (Fig. 7b). The high VPD in the dry season is expected to reduce soil water content through increased soil surface evaporation (Yang et al., 2020). The rubber plantations showed larger ET_c than P during most of the dry season, indicating water deficit (Fig. 7a). Moreover, SM was not a key driver for ET_c and T_c at our site (Fig. 7) and other rubber plantation sites around the world (Guardiola-Claramonte et al., 2008; George et al., 2009; Gonkhamdee et al., 2010; Kobayashi et al., 2014; Niu et al., 2017). Several investigations revealed that rubber trees efficiently use the available water in the deep root zone to avoid severe water stress during the dry season (Guardiola-Claramonte et al., 2010; Liu et al., 2014a,b; Kumagai et al., 2015). Importantly, soil water is extracted from deep layers at the rubber site but is not released by transpiration until new foliage is grown. Therefore, we suggest that SM is not the main water source for trees during the dry season, but SM increase during the FG season can become crucial in extreme drought events when deep soil water is depleted and should be considered in future studies.

5. Conclusion

Fog events and meteorological parameters during FG and non-FG days of cool and hot dry seasons, as well as concurring T_c and WP_c of mature rubber (*H. brasiliensis*) plantations, were studied in detail. The analysis of 3 years of continuous observation showed that fog occurred during 42% of the total study period. During the highly frequent dense fog events in the dry season, Tair often dropped below 5 °C, which triggered leaf shedding of rubber trees and thus they became physiologically less active. Compared with cool dry non-FG days, the presence of fog was associated with lower ET_c rates (15% lower). In addition, net carbon uptake rate is generally low during cool dry season. The dense FG days did not affect GPP, but decreased ET_c, leading to an enhanced WP_c during the FG days compared with the non-FG days of the cool dry season, whereas no significant changes of WP_c were noticed between FG and non-FG days of the hot dry season. Statistical analysis demonstrated that physiological parameters (NEE, GPP, ET_c, WP_c, Gs and T_c) were mainly regulated by the concomitant changes of Tair and VPD during cool dry FG days. The study suggests that low fog occurrence would cause greater dry season demand for groundwater in rubber plantations and decrease ecosystem WP_c. These results highlight the importance of fog, and the relevant processes need to be included in ecosystem modeling. Long-term study is essential to understand local fog climatology. Sustainable management plans should be balanced against the ecological as well as the socioeconomic benefits of rubber plantations, which provide livelihoods to smallholders and their employees. Tropical Asia, particularly SEA, is most likely to face water scarcity and water demand with future droughts linked to large-scale deforestation and global warming (Ismail and Go, 2021), which will increase vulnerability to water scarcity for rubber plantations as well as agricultural crops. In montane areas of SEA, drought in the dry season can be partially relieved by fog occurrence. Our study highlights that during FG days the rubber plantation utilized less water and thus increased the WP_c; therefore, the rubber farmers should implement ET_c-based adaptive irrigation management systems for better yield, particularly during the dry season of the non-FG season. Finally, we also suggest that the irrigation schedule be minimized for other agricultural crops of the region on FG days, which will also help in conserving water to sustain agriculture during the dry season.

CRediT authorship contribution statement

Palingamoorthy Gnanamoorthy: Conceptualization, Investigation, Methodology, Validation, Visualization, Writing – original draft. **Qinghai Song:** Funding acquisition, Project administration, Investigation, Resources, Supervision, Writing – original draft. **Junbin Zhao:** Conceptualization, Validation, Writing – review & editing. **Yiping Zhang:** Supervision, Funding acquisition, Project administration, Writing – original draft. **Jing Zhang:** Methodology. **Youxing Lin:** . **Liguo Zhou:** . **Sadia Bibi:** Writing – review & editing. **Chenna Sun:** . **Hui Yu:** . **Wenjun Zhou:** Writing – review & editing. **Liqing Sha:** Validation, Writing – review & editing. **Shusen Wang:** Methodology, Writing – review & editing. **S. Chakraborty:** Writing – review & editing.

Pramit Kumar Deb Burman: Methodology, Writing – review & editing.

Declaration of Competing Interest

The authors declare that they have no known competing financial interests or personal relationships that could have appeared to influence the work reported in this paper.

Acknowledgments

This work was supported by Xishuangbanna Station for Tropical Rain Forest Ecosystem Studies (XSTRE), China Flux Observation and Research Network (ChinaFlux) and the Public Technology Services Center, Xishuangbanna Tropical Botanical Garden (XTBG), Chinese Academy of Sciences (CAS). This work was funded by the National Natural Science Foundation of China (Grant Nos. 41961144017, 41671209, 31770528), the National Key Research and Development Program of China (Grant No. 2016YFC0502105), Yunnan Province "young and middle aged academic and technical leaders reserve talents" project (202005ac160003), Yunnan Province "ten thousand talents plan youth top talent" project, China Postdoctoral Science Foundation (Grant No. 2019M653512), Orientation training of postdoctoral research in Yunnan Province and CAS Key Laboratory of Tropical Forest Ecology, XTBG, We thank Mr. Donghai Yang for his assistance with the research and fieldwork.

Appendix A. Supplementary data

Supplementary data to this article can be found online at https://doi.org/10.1016/j.jhydrol.2022.128016.

References

Alvarado-Barrientos, M.S., Holwerda, F., Asbjornsen, H., Dawson, T.E., Bruijnzeel, L.A., 2014. Suppression of transpiration due to cloud immersion in a seasonally dry Mexican weeping pine plantation. Agric. For. Meteorol. 186, 12–25. https://doi.org/10.1016/j.agrformet.2013.11.002.

Alvarado-Barrientos, M.S., Holwerda, F., Geissert, D.R., Muñoz-Villers, L.E., Gotsch, S.G., Asbjornsen, H., Dawson, T.E., 2015. Nighttime transpiration in a seasonally dry tropical montane cloud forest environment. Trees 29 (1), 259–274. https://doi.org/10.1007/s00468-014-1111-1.

Aubinet, M., Grelle, A., Ibrom, A., Rannik, Ü., Moncrieff, J., Foken, T., Vesala, T., 1999. Estimates of the Annual Net Carbon and Water Exchange of Forests: The EUROFLUX Methodology. Adv. Ecol. Res. 30 (C), 113–175. https://doi.org/10.1016/S0065-2504(08)60018-5.

Baguskas, S.A., Clemesha, R.E.S., Loik, M.E., 2018. Coastal low cloudiness and fog enhance crop water use efficiency in a California agricultural system. Agric. For. Meteorol. 252, 109–120. https://doi.org/10.1016/j.agrformet.2018.01.015.

Baguskas, S.A., King, J.Y., Fischer, D.T., D'Antonio, C.M., Still, C.J., 2017. Impact of fog drip versus fog immersion on the physiology of Bishop pine saplings. Funct. Plant Biol. 44 (3), 339–350. https://doi.org/10.1071/FP16234.

Baguskas, S.A., Oliphant, A.J., Clemesha, R.E.S., Loik, M.E., 2021. Water and Light-Use Efficiency Are Enhanced Under Summer Coastal Fog in a California Agricultural System. J. Geophys. Res. Biogeosci. 126 (5) https://doi.org/10.1029/2020JG006193.

Baldocchi, D., Valentini, R., Running, S., Oechel, W., Dahlman, R., 1996. Strategies for measuring and modelling carbon dioxide and water vapour fluxes over terrestrial ecosystems. Glob. Chang. Biol. 2, 159–168. https://doi.org/10.1111/j.1365-2486.1996.tb00069.x.

Balasubramanian, D., Zhang, Y.-P., Grace, J., Sha, L.-Q., Jin, Y., Zhou, L.-G., Lin, Y.-X., Zhou, R.-W., Gao, J.-B., Song, Q.-H., Liu, Y.-T., Zhou, W.-J., 2020. Soil organic matter as affected by the conversion of natural tropical rainforest to monoculture rubber plantations under acric ferralsols. Catena 195, 104753.

Berry, Z.C., White, J.C., Smith, W.K., 2014. Foliar uptake, carbon fluxes and water status are affected by the timing of daily fog in saplings from a threatened cloud forest. Tree Physiol. 34 (5), 459–470. https://doi.org/10.1093/treephys/tpu032.

Bittencourt, P.R.L., Barros, F.d.V., Eller, C.B., Müller, C.S., Oliveira, R.S., 2019. The fog regime in a tropical montane cloud forest in Brazil and its effects on water, light and microclimate. Agric. For. Meteorol. 265, 359–369.

Blagodatsky, S., Xu, J., Cadisch, G., 2016. Carbon balance of rubber (*Hevea brasiliensis*) plantations: A review of uncertainties at plot, landscape and production level. Agric. Ecosyst. Environ. 221, 8–19. https://doi.org/10.1016/j.agee.2016.01.025.

Bruijnzeel, L.A., 2001. Hydrology of tropical montane cloud forests: A reassessment. Land Use Water Resour. Res., 1, 1.1-1.18. Retrieved from.

Bruijnzeel, L.A., Mulligan, M., Scatena, F.N., 2011. Hydrometeorology of tropical montane cloud forests: Emerging patterns. Hydrol. Process. 25 (3), 465–498. https://doi.org/10.1002/hyp.7974.

Burba, G., 2013. Eddy Covariance Method for Scientific, Industrial, Agricultural, and Regulatory Applications: A Field Book on Measuring Ecosystem Gas Exchange and Areal Emission Rates. LI-COR Biosciences, Lincoln, NE, USA, p. 331.

Cao, M., Zhang, J., Feng, Z., Deng, J., Deng, X., 1996. Tree species composition of a seasonal rain forest in Xishuangbanna, Southwest China. Tropical Ecol. 37 (2), 183–192.

Chen, J.W., Cao, K.F., 2008. Changes in activities of antioxidative system and monoterpene and photochemical efficiency during seasonal leaf senescence in *Hevea brasiliensis* trees. Acta Physiologiae Plantarum 30 (1), 1–9. https://doi.org/10.1007/s11738-007-0070-1.

Chu, H.-S., Chang, S.-C., Klemm, O., Lai, C.-W., Lin, Y.-Z., Wu, C.-C., Lin, J.-Y., Jiang, J.-Y., Chen, J., Gottgens, J.F., Hsia, Y.-J., 2014. Does canopy wetness matter? Evapotranspiration from a subtropical montane cloud forest in Taiwan. Hydrol. Process. 28 (3), 1190–1214.

Dawson, T.E., Burgess, S.S.O., Tu, K.P., Oliveira, R.S., Santiago, L.S., Fisher, J.B., Simonin, K.A., Ambrose, A.R., 2007. Nighttime transpiration in woody plants from contrasting ecosystems. Tree Physiol. 27 (4), 561–575.

Eller, C.B., Lima, A.L., Oliveira, R.S., 2013. Foliar uptake of fog water and transport belowground alleviates drought effects in the cloud forest tree species, *Drimys brasiliensis* (Winteraceae). New Phytol. 199 (1), 151–162. https://doi.org/10.1111/nph.12248.

Eller, C.B., Lima, A.L., Oliveira, R.S., 2016. Cloud forest trees with higher foliar water uptake capacity and anisohydric behavior are more vulnerable to drought and climate change. New Phytol. 211 (2), 489–501. https://doi.org/10.1111/nph.13952.

Elliott, S., Baker, P.J., Borchert, R., 2006. Leaf flushing during the dry season: The paradox of Asian monsoon forests. Glob. Ecol. Biogeogr. 15 (3), 248–257. https://doi.org/10.1111/j.1466-8238.2006.00213.x.

Eugster, W., Burkard, R., Holwerda, F., Scatena, F.N., Bruijnzeel, L.A., 2006. Characteristics of fog and fogwater fluxes in a Puerto Rican elfin cloud forest. Agric. For. Meteorol. 139 (3–4), 288–306. https://doi.org/10.1016/j.agrformet.2006.07.008.

Ewers, B.E., Oren, R., 2000. Analysis of assumptions and errors in the calculation of stomatal conductance from sap flux measurements. Tree Physiol. 20, 579–589. https://doi.org/10.1093/treephys/20.9.579.

Falge, E., Baldocchi, D., Olson, R., Anthoni, P., Aubinet, M., Bernhofer, C., Burba, G., Ceulemans, R., Clement, R., Dolman, H., Granier, A., Gross, P., Grünwald, T., Hollinger, D., Jensen, N.-O., Katul, G., Keronen, P., Kowalski, A., Lai, C.T., Law, B.E., Meyers, T., Moncrieff, J., Moors, E., Munger, J.W., Pilegaard, K., Rannik, Ü., Rebmann, C., Suyker, A., Tenhunen, J., Tu, K., Verma, S., Vesala, T., Wilson, K., Wofsy, S., 2001. Gap filling strategies for defensible annual sums of net ecosystem exchange. Agric. For. Meteorol. 107 (1), 43–69.

Fei, X., Song, Q., Zhang, Y., Liu, Y., Sha, L., Yu, G., Zhang, L., Duan, C., Deng, Y., Wu, C., Lu, Z., Luo, K., Chen, A., Xu, K., Liu, W., Huang, H., Jin, Y., Zhou, R., Li, J., Lin, Y., Zhou, L., Fu, Y., Bai, X., Tang, X., Gao, J., Zhou, W., Grace, J., 2018. Carbon exchanges and their responses to temperature and precipitation in forest ecosystems in Yunnan, Southwest China. Sci. Total Environ. 616-617, 824–840.

Fernández, J.E., Alcon, F., Diaz-Espejo, A., Hernandez-Santana, V., Cuevas, M.V., 2020. Water use indicators and economic analysis for on-farm irrigation decision: A case study of a super high density olive tree orchard. Agric. Water Manage. 237 (1), 106074 https://doi.org/10.1016/j.agwat.2020.106074.

Fox, J., Castella, J.C., Ziegler, A.D., 2014. Swidden, rubber and carbon: Can REDD+ work for people and the environment in Montane Mainland Southeast Asia? Global Environ. Change 29, 318–326. https://doi.org/10.1016/j.gloenvcha.2013.05.011.

Fu, P.L., Liu, W.J., Fan, Z.X., Cao, K.F., 2016. Is fog an important water source for woody plants in an Asian tropical karst forest during the dry season? Ecohydrology 9 (6), 964–972. https://doi.org/10.1002/eco.1694.

García-Santos, G., Bruijnzeel, L.A., 2011. Rainfall, fog and throughfall dynamics in a subtropical ridge top cloud forest, National Park of Garajonay (La Gomera, Canary Islands, Spain). Hydrol. Process. 25 (3), 411–417. https://doi.org/10.1002/hyp.7760.

George, S., Suresh, P.R., Wahid, P.A., Nair, R.B., Punnoose, K.I., 2009. Active root distribution pattern of *Hevea brasiliensis* determined by radioassay of latex serum. Agrofor. Syst. 76 (2), 275–281. https://doi.org/10.1007/s10457-008-9104-y.

Gerlein-Safdi, C., Gauthier, P.P.G., Caylor, K.K., 2018a. Dew-induced transpiration suppression impacts the water and isotope balances of Colocasia leaves. Oecologia 187 (4), 1041–1051. https://doi.org/10.1007/s00442-018-4199-y.

Gerlein-Safdi, C., Koohafkan, M.C., Chung, M., Rockwell, F.E., Thompson, S., Caylor, K. K., 2018b. Dew deposition suppresses transpiration and carbon uptake in leaves. Agric. For. Meteorol. 259, 305–316. https://doi.org/10.1016/j.agrformet.2018.05.015.

Giambelluca, T.W., Mudd, R.G., Liu, W., Ziegler, A.D., Kobayashi, N., Kumagai, T., Miyazawa, Y., Lim, T.K., Huang, M., Fox, J., Yin, S., Mak, S.V., Kasemsap, P., 2016. Evapotranspiration of rubber (*Hevea brasiliensis*) cultivated at two plantation sites in Southeast Asia. Water Resour. Res. 52 (2), 660–679.

Gonkhamdee, S., Maeght, J.-L., Do, F., Pierret, A., 2010. Growth dynamics of fine *Hevea brasiliensis* roots along a 4.5-m soil profile. Khon Kaen Agricul. J. 37 (2552), 265–276.

Gotsch, S.G., Asbjornsen, H., Holwerda, F., Goldsmith, G.R., Weintraub, A.E., Dawson, T. E., 2014. Foggy days and dry nights determine crown-level water balance in a seasonal tropical montane cloud forest. Plant, Cell Environ. 37 (1), 261–272. https://doi.org/10.1111/pce.12151.

Granier, A., 1985. Une nouvelle méthode pour la mesure du flux de sève brute dans le tronc des arbres. Annales Des Sciences Forestières 42 (2), 193–200. https://doi.org/10.1051/forest:19850204.
Granier, A., 1987. Evaluation of transpiration in a Douglas-fir stand by means of sap flow measurements. Tree Physiol. 3 (4), 309–320. https://doi.org/10.1093/treephys/3.4.309.
Guardiola-Claramonte, M., Troch, P.A., Ziegler, A.D., Giambelluca, T.W., Vogler, J.B., Nullet, M.A., 2008. Local hydrologic effects of introducing non-native vegetation in a tropical catchment. Ecohydrology 1 (1), 13–22. https://doi.org/10.1002/eco.3.
Guardiola-Claramonte, M., Troch, P.A., Ziegler, A.D., Giambelluca, T.W., Durcik, M., Vogler, J.B., Nullet, M.A., 2010. Hydrologic effects of the expansion of rubber (*Hevea brasiliensis*) in a tropical catchment. Ecohydrology 3 (3), 306–314. https://doi.org/10.1002/eco.110.
Hauser, I., Martin, K., Germer, J., He, P., Blagodatskiy, S., Liu, H., … Cadisch, G. (2015). Environmental and socio-economic impacts of rubber cultivation in the Mekong region: Challenges for sustainable land use. *CAB Reviews: Perspectives in Agriculture, Veterinary Science, Nutrition and Natural Resources*. CABI International. https://doi.org/10.1079/PAVSNNR201510027.
Hales, S., 1757. Vegetable staticks. Isaac Newton, London, UK.
Hardanto, A., Röll, A., Niu, F., Meijide, A., Hendrayanto, Hölscher, D., 2017. Oil palm and rubber tree water use patterns: Effects of topography and flooding. Front. Plant Sci. 8 https://doi.org/10.3389/fpls.2017.00452.
Hildebrandt, A., Al Aufi, M., Amerjeed, M., Shammas, M., Eltahir, E.A.B., 2007. Ecohydrology of a seasonal cloud forest in Dhofar: 1. Field experiment. Water Resour. Res. 43 (10) https://doi.org/10.1029/2006WR005261.
Hutley, L.B., Doley, D., Yates, D.J., Boonsaner, A., 1997. Water balance of an Australian subtropical rainforest at altitude: The ecological and physiological significance of intercepted cloud and fog. In Austr. J. Botany 45, 311–329. https://doi.org/10.1071/BT96014.
Isarangkool Na Ayutthaya, S., Do, F.C., Pannangpetch, K., Junjittakarn, J., Maeght, J.-L., Rocheteau, A., Cochard, H., 2011. Water loss regulation in mature *Hevea brasiliensis*: Effects of intermittent drought in the rainy season and hydraulic regulation. Tree Physiol. 31 (7), 751–762.
Ismail, Z., Go, Y.I., 2021. Fog-to-Water for Water Scarcity in Climate-Change Hazards Hotspots: Pilot Study in Southeast Asia. Global Challenges 5 (5), 2000036. https://doi.org/10.1002/gch2.202000036.
Jiang, X.J., Chen, C., Zhu, X., Zakari, S., Singh, A.K., Zhang, W., Zeng, H., Yuan, Z.-Q., He, C., Yu, S., Liu, W., 2019. Use of dye infiltration experiments and HYDRUS-3D to interpret preferential flow in soil in a rubber-based agroforestry systems in Xishuangbanna, China. Catena 178, 120–131.
Kijne, J. W., Barker, R., Molden. D. (Eds.) 2003. Water productivity in agriculture: limits and opportunities for improvement. Wallingford, UK: CABI; Colombo, Sri Lanka: International Water Management Institute (IWMI). xix, 332p. (Comprehensive Assessment of Water Management in Agriculture Series 1).
Kobayashi, N., Kumagai, T., Miyazawa, Y., Matsumoto, K., Tateishi, M., Lim, T.K., Mudd, R.G., Ziegler, A.D., Giambelluca, T.W., Yin, S., 2014. Transpiration characteristics of a rubber plantation in central Cambodia. Tree Physiol. 34 (3), 285–301.
Kumagai, T., Mudd, R.G., Giambelluca, T.W., Kobayashi, N., Miyazawa, Y., Lim, T.K., Liu, W., Huang, M., Fox, J.M., Ziegler, A.D., Yin, S., Mak, S.V., Kasemsap, P., 2015. How do rubber (*Hevea brasiliensis*) plantations behave under seasonal water stress in northeastern Thailand and central Cambodia? Agric. For. Meteorol. 213, 10–22.
Lenth, R. V., Buerkner, P., Herve, M., Love, J., Riebl, H., & Singmann, H. (2021). Package 'emmeans'. https://cran.r-project.org/web/packages/emmea ns/emmea ns.pdf.
Lin, Y.X., Zhang, Y.P., Zhao, W., Zhang, X., Dong, Y.X., Fei, X.H., Li, J., 2016. Comparison of transpiration characteristics in different aged rubber plantations. Chinese J. Ecol. 35 (4), 855–863. https://doi.org/10.13292/j.l000-4890.201604.006.
Lin, Y., Grace, J., Zhao, W., Dong, Y., Zhang, X., Zhou, L., Fei, X., Jin, Y., Li, J., Nizami, S. M., Balasubramanian, D., Zhou, W., Liu, Y., Song, Q., Sha, L., Zhang, Y., 2018a. Water-use efficiency and its relationship with environmental and biological factors in a rubber plantation. J. Hydrol. 563, 273–282.
Lin, Y., Zhang, Y., Zhao, W., Dong, Y., Fei, X., Song, Q., Sha, L., Wang, S., Grace, J., 2018b. Pattern and driving factor of intense defoliation of rubber plantations in SW China. Ecol. Ind. 94, 104–116.
Liu, W., Li, J., Lu, H., Wang, P., Luo, Q., Liu, W., Li, H., 2014a. Vertical patterns of soil water acquisition by non-native rubber trees (*Hevea brasiliensis*) in Xishuangbanna, southwest China. Ecohydrology 7 (4), 1234–1244. https://doi.org/10.1002/eco.1456.
Liu, W., Li, P., Duan, W., Liu, W., 2014b. Dry-season water utilization by trees growing on thin karst soils in a seasonal tropical rainforest of Xishuangbanna, Southwest China. Ecohydrology 7 (3), 927–935. https://doi.org/10.1002/eco.1419.
Liu, W., Meng, F.R., Zhang, Y., Liu, Y., Li, H., 2004. Water input from fog drip in the tropical seasonal rain forest of Xishuangbanna, South-West China. J. Trop. Ecol. 20 (5), 517–524. https://doi.org/10.1017/S0266467404001890.
Ludwig, F., Jewitt, R.A., Donovan, L.A., 2006. Nutrient and water addition effects on day- and night-time conductance and transpiration in a C3 desert annual. Oecologia 148 (2), 219–225. https://doi.org/10.1007/s00442-006-0367-6.
Ma, X., Lacombe, G., Harrison, R., Xu, J., van Noordwijk, M., 2019. Expanding rubber plantations in Southern China: Evidence for hydrological impacts. Water 11 (4), 651. https://doi.org/10.3390/w11040651.
Mercado, L.M., Bellouin, N., Sitch, S., Boucher, O., Huntingford, C., Wild, M., Cox, P.M., 2009. Impact of changes in diffuse radiation on the global land carbon sink. Nature 458 (7241), 1014–1017. https://doi.org/10.1038/nature07949.
Mildenberger, K., Beiderwieden, E., Hsia, Y.-J., Klemm, O., 2009. CO_2 and water vapor fluxes above a subtropical mountain cloud forest—The effect of light conditions and fog. Agric. For. Meteorol. 149, 1730–1736. https://doi.org/10.1016/j.agrformet.2009.06.004.
Molden, D., 1997. Accounting for Water Use and Productivity. SWIM Paper 1. IIMI, Colombo.
Myers, N., Mittermeler, R.A., Mittermeler, C.G., Da Fonseca, G.A.B., Kent, J., 2000. Biodiversity hotspots for conservation priorities. Nature 403 (6772), 853–858. https://doi.org/10.1038/35002501.
National oceanic and atmospheric administration (NOAA)., 1995. Surface observations and reports, Office of the federal coordinator for meteorological services and supporting research Federal meteorological handbook number 1, FCM-H1-1995 Washington, DC, available at: http://marrella.meteor.wisc.edu/aos452/fmh1.pdf.
Navarrete, C.B., 2020. Package "Dominanceanalysis". https://cran.r-project.org/web/packages/dominanceanalysis/dominanceanalysis.pdf.
Niu, F., Röll, A., Meijide, A., Hendrayanto, Hölscher, D., 2017. Rubber tree transpiration in the lowlands of Sumatra. Ecohydrology 10 (7), e1882.
Noormets, A., Gavazzi, M.J., McNulty, S.G., Domec, J.C., Sun, G., King, J.S., Chen, J., 2010. Response of carbon fluxes to drought in a coastal plain loblolly pine forest. Glob. Change Biol. 16 (1), 272–287. https://doi.org/10.1111/j.1365-2486.2009.01928.x.
Pfeifer, M., Kor, L., Nilus, R., Turner, E., Cusack, J., Lysenko, I., Khoo, M., Chey, V.K., Chung, A.C., Ewers, R.M., 2016. Mapping the structure of Borneo's tropical forests across a degradation gradient. Remote Sens. Environ. 176, 84–97.
Priyadarshan, P.M., 2011. Biology of Hevea rubber. Biology of Hevea Rubber (pp. 1–226). CABI Publishing, Preston, UK. https://doi.org/10.1079/9781845936662.0000.
R Core Team, 2019. *R: A language and environment for statistical computing*. R Foundation for Statistical Computing. http://www.R-project.org/.
Ramírez, D.A., Yactayo, W., Rolando, J.L., Quiroz, R., 2018. Preliminary Evidence of Nocturnal Transpiration and Stomatal Conductance in Potato and their Interaction with Drought and Yield. Am. J. Potato Res. 95 (2), 139–143. https://doi.org/10.1007/s12230-017-9618-9.
Regalado, C.M., Ritter, A., 2007. An alternative method to estimate zero flow temperature differences for Granier's thermal dissipation technique. Tree Physiol. 27 (8), 1093–1102. https://doi.org/10.1093/treephys/27.8.1093.
Reichstein, M., Falge, E., Baldocchi, D., Papale, D., Aubinet, M., Berbigier, P., Bernhofer, C., Buchmann, N., Gilmanov, T., Granier, A., Grunwald, T., Havrankova, K., Ilvesniemi, H., Janous, D., Knohl, A., Laurila, T., Lohila, A., Loustau, D., Matteucci, G., Meyers, T., Miglietta, F., Ourcival, J.-M., Pumpanen, J., Rambal, S., Rotenberg, E., Sanz, M., Tenhunen, J., Seufert, G., Vaccari, F., Vesala, T., Yakir, D., Valentini, R., 2005. On the separation of net ecosystem exchange into assimilation and ecosystem respiration: Review and improved algorithm. Glob. Change Biol. 11 (9), 1424–1439.
Ritter, A., Regalado, C.M., 2017. Tree stomata conductance estimates of a wax myrtle-tree heath (fayal-brezal) cloud forest as affected by fog. Agricul. Forest Meteorol. 247, 116–130. https://doi.org/10.1016/j.agrformet.2017.07.021.
Ritter, A., Regalado, C.M., Aschan, G., 2009. Fog reduces transpiration in tree species of the Canarian relict heath-laurel cloud forest (Garajonay National Park, Spain). Tree Physiol. 29 (4), 517–528. https://doi.org/10.1093/treephys/tpn043.
Rusli, N., Majid, M.R., 2014. Monitoring and mapping leaf area index of rubber and oil palm in small watershed area. In IOP Conference Series: Earth and Environmental Science (Vol. 18). Institute of Physics Publishing. https://doi.org/10.1088/1755-1315/18/1/012036.
Röll, A., Niu, F., Meijide, A., Ahongshangbam, J., Ehbrecht, M., Guillaume, T., Gunawan, D., Hardanto, A., Hendrayanto, Hertel, D., Kotowska, M.M., Kreft, H., Kuzyakov, Y., Leuschner, C., Nomura, M., Polle, A., Rembold, K., Sahner, J., Seidel, D., Zemp, D.C., Knohl, A., Hölscher, D., 2019. Transpiration on the rebound in lowland Sumatra. Agric. For. Meteorol. 274, 160–171.
Sabbatini, S., Mammarella, I., Arriga, N., Fratini, G., Graf, A., Hörtnagl, L., Ibrom, A., Papale, D., 2018. Eddy covariance raw data processing for CO_2 and energy fluxes calculation at ICOS ecosystem stations. Int. Agrophys. 32 (4), 495–515. https://doi.org/10.1515/intag -2017-0043.
Saleska, S.R., Miller, S.D., Matross, D.M., Goulden, M.L., Wofsy, S.C., da Rocha, H.R., de Camargo, P.B., Crill, P., Daube, B.C., de Freitas, H.C., Hutyra, L., Keller, M., Kirchhoff, V., Menton, M., Munger, J.W., Pyle, E.H., Rice, A.H., Silva, H., 2003. Carbon in Amazon Forests: Unexpected Seasonal Fluxes and Disturbance-Induced Losses. Science 302 (5650), 1554–1557.
Song, Q.-H., Tan, Z.-H., Zhang, Y.-P., Sha, L.-Q., Deng, X.-B., Deng, Y., Zhou, W.-J., Zhao, J.-F., Zhao, J.-B., Zhang, X., Zhao, W., Yu, G.-R., Sun, X.-M., Liang, N.-S., Yang, L.-Y., 2014. Do the rubber plantations in tropical China act as large carbon sinks? IForest 7 (1), 42–47.
Stone, E.C., 1957. Dew as an Ecological Factor: I. A Review of the Literature. Ecology 38 (3), 407–413. https://doi.org/10.2307/1929883.
Tan, Z.-H., Zhang, Y.-P., Song, Q.-H., Liu, W.-J., Deng, X.-B., Tang, J.-W., Deng, Y., Zhou, W.-J., Yang, L.-Y., Yu, G.-R., Sun, X.-M., Liang, N.-S., 2011. Rubber plantations act as water pumps in tropical China. Geophys. Res. Lett. 38 (24), n/a–n/a.
Tan, Z., Zhang, Y., Yu, G., Sha, L., Tang, J., Deng, X., Song, Q., 2010. Carbon balance of a primary tropical seasonal rain forest. J. Geophys. Res. Atmos. 115 (13) https://doi.org/10.1029/2009JD012913.
Tanner, C.B., Thurtell, G.W., 1969. Anemoclinometer Measurements of Reynolds Stress and Heat Transport in the Atmospheric Surface Layer, 82. University of Wisconsin, Madison, Wisconsin.
Tardif, R., Rasmussen, R.M., 2007. Event-based climatology and typology of fog in the New York City region. J. Appl. Meteorol. Climatol. 46 (8), 1141–1168. https://doi.org/10.1175/JAM2516.1.
Teuling, A.J., Troch, P.A., 2005. Improved understanding of soil moisture variability dynamics. Geophys. Res. Lett. 32 (5), 1–4. https://doi.org/10.1029/2004GL021935.

Vasey, M.C., Loik, M.E., Parker, V.T., 2012. Influence of summer marine fog and low cloud stratus on water relations of evergreen woody shrubs (Arctostaphylos: Ericaceae) in the chaparral of central California. Oecologia 170 (2), 325–337. https://doi.org/10.1007/s00442-012-2321-0.

Vautard, R., Yiou, P., Van Oldenborgh, G.J., 2009. Decline of fog, mist and haze in Europe over the past 30 years. Nat. Geosci. 2 (2), 115–119. https://doi.org/10.1038/ngeo414.

Vogel, A.W., Wang, M.Z., & Huang, X.Q., 1995. People's Republic of China: reference soil (lotosal) of tropical southern Yunnan province. Institute of soil science–Academica Sinica, Nanjing, and International soil reference and information centre, Wageningen.

Wang, W., Liao, Y., Wen, X., Guo, Q., 2013. Dynamics of CO_2 fluxes and environmental responses in the rain-fed winter wheat ecosystem of the Loess Plateau, China. Sci. Total Environ. 461–462, 10–18. https://doi.org/10.1016/j.scitotenv.2013.04.068.

Warren-Thomas, E.M., Edwards, D.P., Bebber, D.P., Chhang, P., Diment, A.N., Evans, T. D., Lambrick, F.H., Maxwell, J.F., Nut, M., O'Kelly, H.J., Theilade, I., Dolman, P.M., 2018. Protecting tropical forests from the rapid expansion of rubber using carbon payments. Nature Commun. 9 (1) https://doi.org/10.1038/s41467-018-03287-9.

Webb, E.K., Pearman, G.I., Leuning, R., 1980. Correction of flux measurements for density effects due to heat and water vapour transfer. Q. J. R. Meteorol. Soc. 106 (447), 85–100. https://doi.org/10.1002/qj.49710644707.

Wickham, H., 2016. ggplot2; Elegant graphics for data analysis (Use R!). Springer, 213 pp. http://had.co.nz/ggplo t2/book.

Wilczak, J.M., Oncley, S.P., Stage, S.A., 2001. Sonic anemometer tilt correction algorithms. Bound.-Layer Meteorol. 99 (1), 127–150. https://doi.org/10.1023/A:10189 66204465.

Witiw, M.R., LaDochy, S., 2008. Trends in fog frequencies in the Los Angeles Basin. Atmos. Res. 87 (3–4), 293–300. https://doi.org/10.1016/j.atmosres.2007.11.010.

Wutzler, T., Lucas-Moffat, A., Migliavacca, M., Knauer, J., Sickel, K., Šigut, L., Menzer, O., Reichstein, M., 2018. Basic and extensible post-processing of eddy covariance flux data with REddyProc. Biogeosciences 15 (16), 5015–5030. https://doi.org/10.5194/bg-15-5015-2018.

Xu, J., Grumbine, R.E., Beckschäfer, P., 2014. Landscape transformation through the use of ecological and socioeconomic indicators in Xishuangbanna, Southwest China, Mekong Region. Ecol. Ind. 36, 749–756. https://doi.org/10.1016/j.ecolind.2012.08.023.

Yang, B., Meng, X., Singh, A.K., Wang, P., Song, L., Zakari, S., Liu, W., 2020. Intercrops improve surface water availability in rubber-based agroforestry systems. Agric. Ecosyst. Environ. 298, 106937 https://doi.org/10.1016/j.agee.2020.106937.

Yokoyama, G., Yasutake, D., Minami, K., Kimura, K., Marui, A., Yueru, W.u., Feng, J., Wang, W., Mori, M., Kitano, M., 2021. Evaluation of the physiological significance of leaf wetting by dew as a supplemental water resource in semi-arid crop production. Agric. Water Manage. 255, 106964.

Yu, G.R., Wen, X.F., Sun, X.M., Tanner, B.D., Lee, X., Chen, J.Y., 2006. Overview of ChinaFLUX and evaluation of its eddy covariance measurement. Agric. For. Meteorol. 137 (3–4), 125–137. https://doi.org/10.1016/j.agrformet.2006.02.011.

Zakari, S., Liu, W., Wu, J., Singh, A.K., Jiang, X., Yang, B., Chen, C., Zhu, X., 2020. Decay and erosion-related transport of sulfur compounds in soils of rubber based agroforestry. J. Environ. Manage. 274, 111200.

Zhang, Y.J., Holbrook, N.M., Cao, K.F., 2014. Seasonal dynamics in photosynthesis of woody plants at the northern limit of Asian tropics: Potential role of fog in maintaining tropical rainforests and agriculture in Southwest China. Tree Physiol. 34 (10), 1069–1078. https://doi.org/10.1093/treephys/tpu083.

Zhao, W., Zhang, Y.P., Song, Q.H., Zhang, X., Ji, H.L., Syed Moazzam, N., Yu, L., 2014. Characteristics of transpiration of rubber trees (*Hevea brasiliensis*) and its relationship with environmental factors. Chin. J. Ecol. 33 (7), 1803–1810.

Zhou, S., Yu, B., Huang, Y., Wang, G., 2015. Daily underlying water use efficiency for AmeriFlux sites. J. Geophys. Res. Biogeosci. 120 (5), 887–902. https://doi.org/10.1002/2015JG002947.

Zhou, W.-J., Ji, H.-l., Zhu, J., Zhang, Y.-P., Sha, L.-Q., Liu, Y.-T., Zhang, X., Zhao, W., Dong, Y.-X., Bai, X.-L., Lin, Y.-X., Zhang, J.-H., Zheng, X.-H., 2016. The effects of nitrogen fertilization on N2O emissions from a rubber plantation. Sci. Rep. 6 (1) https://doi.org/10.1038/srep28230.

Zhu, H., Xu, Z.F., Wang, H., Li, B.G., 2004. Tropical rain forest fragmentation and its ecological and species diversity changes in southern Yunnan. Biodivers. Conserv. 13 (7), 1355–1372. https://doi.org/10.1023/B:BIOC.0000019397.98407.c3.

Zongdao, H., and Xueqin, Z. 1983. Rubber cultivation in China. Proceedings, Rubber Research Institute of Malaysia, Planters' Conference, 1983, Kuala Lumpur, Malaysia, pp. 31-43.